Sudan University of Science and Technology

College of Graduate Studies

Preparation, Characterization and Functional Properties of Nickel Nanoparticles (NiNPs)

تحضير وتشخيص والخصائص الوظيفية لجسيمات النيكل النانوية

A Thesis submitted in fulfillment of the requirement for the degree of Ph.D. in Chemistry.

By

Moaz Siddig Suliman Mohamed (M.Sc. Chemistry)

Supervisor: Prof. Mohammed Elmubark Osman

November, 2021

إستهلال

قال تعالي: **وَقُلِ اعْمَلُوا فَسَيَرَى اللَّهُ عَمَلَكُمْ وَرَسُولُهُ وَالْمُؤْمِنُونَ ۖ وَسَتُرَدُّونَ إِلَىٰ عَالِمِ الْغَيْبِ وَالشَّهَادَةِ فَيُنَبِّئُكُمْ بِمَا كُنْتُمْ تَعْمَلُونَ ﴿105﴾**

صدق الله العظيم

(سورة التوبة - 105)

قال تعالي: **وَمِنَ النَّاسِ وَالدَّوَابِّ وَالْأَنْعَامِ مُخْتَلِفٌ أَلْوَانُهُ كَذَٰلِكَ ۗ إِنَّمَا يَخْشَى اللَّهَ مِنْ عِبَادِهِ الْعُلَمَاءُ ۗ إِنَّ اللَّهَ عَزِيزٌ غَفُورٌ ﴿28﴾**

صدق الله العظيم

(سورة فاطر-28)

Dedication

To my;

Parents,

Brothers,

Sister,

Wife

and friends.

ACKNOWLEDGEMENT

First of all, I would like to thank Allah Almighty for giving me the health and strength to complete this work.

Also, sincere thanks and gratitude to my supervisor **Prof. Mohammed Elmubark Osman**, for his motivation and constructive criticism throughout the course of the project.

My appreciation is due to **Dr. Sahl Yasin** and **Hiba Hashim** from Sudan University of Science and Technology. **Murtada Ahmed** form materials research center, **Mohamed Siddig Suliman**, and **Eman Mahmoud** from The National Researches Center, for their technical support.

List of Abbreviations

(NP) Nanoparicles.

(NiNPs) Nickel nanoparticles.

(NiONPs) Nickel oxide nanoparticles.

(OBNs) Oil-based nanofluids.

(WGSR) Water gas shift reaction.

(EVA) Ethylene-co-vinyl acetate.

(USEPA) United states environmental protection agency.

(CPIs) Corrugated plate interceptors.

(JCPDS) Joint committee of powder diffraction standards.

(TEM) Transmission electron microscope.

(TGA) Thermo-gravimetric analysis.

(DSC) Differential scanning calorimetry analysis.

(rpm) rotate per min.

(SG) Specific gravity.

(API) American petroleum institute number.

Abstract

In the present study, Nickel nanoparticles (NiNPs) were synthesized using Nickel (II)chloride hexahydrate ($NiCl_2 \cdot 6H_2O$) as a precursor and hydrazine monohydrate ($N_2|H_4 \cdot H_2O$) as a reducing agent with different molar ratios of 10 and 15 (N_2H_4/Ni^{2+}) in absolute ethanol at 60 °C. the yield was 90 % for both ratios. The as-obtained samples were characterized using (XRD), (TEM), (TGA-DSC) and (FTIR) spectroscopy. XRD studies confirmed that the synthesized nickel is highly crystalline with face centered cubic structure(fcc). TEM images revealed the formation of a nickel star-like shape when the molar ratio was 10 with an average size of 70-90 nm, and when the molar ratio was 15, a spherical particles shape with an average size of 50-80 nm. TGA-DSC revealed that nickel powders have an oxidization temperature of about 410 °C. FTIR showed absorption band at around 550-600 cm^{-1}. Nickel nanoparticles (NiNPs) were used as catalyst to reduce heavy crude oil viscosity, results showed that 0.05 % NiNPs reduce heavy oil viscosity by ~ 51% evidenced by a slight change in density and API number of 1 % and 9.0% respectively. Results of Nickel nanoparticles (NiNPs) as an adsorbent in produced water treatment show that maximum removal of dissolved oil is 98 %. The adsorption data was inserted into Langmuir and Freundlich's isotherms to obtain adsorption parameters and adsorption capacity of NiNPs. Under Langmuir's isotherm, maximum monolayer adsorption capacity (q_{max}), K_L, R_L and R^2 were 22,841 mg g^{-1}, 0.001121 (L mg^{-1}), 0.670 and 0.9775 respectively. in Freundlich's isotherm model, the constants k, 1/n and R^2 were 24.24, 1.005 and 0.9832 respectively.

المستخلص

في هذه الدراسة ، تم تصنيع جسيمات النيكل النانوية (NiNPs) بإستخدام سداسي هيدرات كلوريد النيكل ($NiCl2 \cdot 6H2O$) وهيدرازين أحادي الهيدرات ($N_2 H_4 \cdot H_2O$) كعامل اختزال بنسب مولارية مختلفة من 10 و 15 (N_2H_4/ Ni^{2+}) في الإيثانول المطلق عند 60 درجة مئوية. كان العائد 90٪ لكلا النسبتين. تم تشخيص العينات التي تم الحصول عليها بإستخدام التحليل الطيفي (XRD) و (TEM) و ((TGA-DSC) و (FTIR) . أكدت دراسات XRD أن النيكل المُصنَّع شديد التبلور مع بنية مكعبة مركزية الوجه .كشفت صور TEM عن تكوين شكل يشبه نجم النيكل عندما كانت النسبة المولية 10 بمتوسط حجم 70-90 نانومتر ، وعندما كانت النسبة المولية 15 ، تشكلت جزيئات كروية بمتوسط حجم 50-80 نانومتر. كشفت TGA-DSC أن مساحيق النيكل لها درجة حرارة أكسدة تبلغ حوالي 410 درجة مئوية. أظهر FTIR نطاق امتصاص عند حوالي 550-600 سم $^{-1}$. تم استخدام جزيئات النيكل النانوية (NiNPs) كمحفز لتقليل لزوجة الزيت الخام الثقيل ، وأظهرت النتائج أن 0.05٪ (NiNPs) تقلل لزوجة الزيت الثقيل بنسبة 51٪ تقريبًا ، كما يتضح من تغير طفيف في الكثافة ورقم API بنسبة 1٪ و 9.0٪ على التوالي. تظهر نتائج جزيئات النيكل النانوية (NiNPs) في معالجة المياه المنتجة أن الحد الأقصى لإزالة الزيت المذاب هو 98٪. تم إدخال بيانات الامتزاز في متساوي الحرارة لانجمويز وفريوندليش للحصول على معلمات الامتزاز وقدرة (NiNPs) في الامتزاز .تحت متساوي الحرارة لانجمويز ، كانت السعة القصوى للامتصاص أحادي الطبقة (q_{max})، K_L، R_L و R2 22,841 mg g^{-1}، (0.001121 (L mg^{-1}) ، 0.670 و 0.9775 على التوالي. في نموذج متساوي الحرارة لـفريوندليش، كانت الثوابت k و n / 1 و R^2 هي 24.24 و 1.005 و 0.9832 على التوالي.

Table of Contents

List of Tables

List of Figures

Chapter One

Introduction and Literature Review

Chapter One

1. Introduction and literature review

1.3 Nanoscience and Nanotechnology

History of nanoscience and nanotechnology reference is, often, made to a lecture given by Richard Feynman in 1959 at Caltech. Entitled "there is plenty of room at the bottom". In his talk, Feynman considered the possibility of, direct, manipulation of individual atoms as a powerful form of synthetic chemistry than those used at the time (Feynman, 1959). Feynman invented that the germ of the idea of the assembler concept that Eric Drexler elaborated in 1980. The assembler refers to a universal nanoscale machine, which makes nanostructure materials (Drexler, 1986).

The royal society and royal academy of engineering defined "nanoscience" as the study of phenomena and manipulation of materials at atomic, molecular, and macro-molecular scales while nanotechnology has been defined as the design, characterization, production, and application of structures, devices and systems by controlling shape and size at nanometer scale (Aslan *et al*., 2005). A more generalized description of nanotechnology is the manipulation of matter with at least one dimension of size from 1 to 100 nanometers, namely, nanomaterials. Intriguingly, these nanomaterials embody distinctive physicochemical and biological properties compared to their conventional counter parts which endow them their beneficial characteristics (Gatoo *et al*., 2014).

Another definition is the "design, characterization, production, and application of materials, devices, and systems by controlling shape and size at the nanoscale" (Ramsden, 2018).

1.4 Nanomaterials

1.4.1 Definitions of Nanomaterials

There are many differences between international agencies on the definition of nanomaterials. In ISO/TS 80004, Nanomaterial is defined as a "material with any external dimension in the nanoscale or having internal or surface structure in the nanoscale", with nanoscale defined as the "length range approximately from 1 nm to 100 nm". This includes both nano-objects, which are discrete pieces of material, and nanostructured materials, which have internal or surface structure on the nanoscale materials in range from 1 to 100 nm in size are called nanomaterials. The noticeable interest of a wide range of researchers on Nanomaterials is due to the infinite and extraordinary properties that they offer when manipulated at the atomic scale. It has been found that materials in nano scale show a very interesting difference in their mechanical and chemical properties (Iso.org, 2018).

The European Commission, adopted definition of Nanomaterials is; "A natural, incidental or manufactured material containing particles, in an unbound state or as an aggregate or as an agglomerate and for 50% or more of the particles in the number size distribution, one or more external dimensions is in the size range 1 nm – 100 nm" (Ec.europa.eu, 2018).

Nanomaterials are generally considered to be a number of atoms or molecules bonded together with a radius of < l00 nm. A nanometer is $l0^{-9}$m or l0 Å, so particles having a radius of about ≤1000 Å, are considered to be nanoparticles (Poole *et al*., 2003).

1.4.2 **Nanomaterials properties**

Comparing to bulk, materials in nanoscale have very unique properties. That uniqueness comes from nanomaterials' size, shape, surface area, composition and so forth (Gatoo *et al*., 2014). Several properties of solids depend mainly on their size over which they are measured. When these measurements are made in nanometer scale, many properties of materials change noticeably, such as melting point,

fluorescence, electrical conductivity, magnetic permeability, and chemical reactivity change as a function of the particle size (Poole *et al*., 2003).

There are two major types of size-dependent effects; the first ones are which related to the fraction of atoms at the surface of the material, and the second ones are quantum effects which show discontinuous behavior due to completion of shell, in systems, with delocalized electrons (Roduner, 2006).

1.2.2.1 Surface effects

Particle in sphere form, its surface scales with the square of its radius *r*, its volume scales with r^3, the total number of atoms *N* scale linearly with volume. And the fraction of atoms at the surface (dispersion F) scales with surface area divided by volume, with the inverse radius or diameter, and thus also with $N^{1/3}$. Accordingly, Atoms at the surface of nanoparticles have a very few neighbors than atoms in the bulk form. Therefore, surface atoms are less stabilized in nanoparticles than bulk due to low coordination and unsatisfied bond. When the particle is small, the fraction of atoms at surface is large. Besides, Surface-to-volume ratio scales with the inverse size, according to that, many properties scales with the same scaling law, such as melting and other phase transition temperatures. Small clusters behave more like molecules than a bulk, and there are many other concepts of thermodynamics which can break down, specially, when the system is small isolated cluster with few atoms (Roduner, 2006).

1.2.2.2 Quantum size effects.

Quantum confinement can be observed once the diameter of a material is of the same magnitude as the de Broglie wavelength of the electron wave function, equation (1-1):

$$\lambda = \frac{h}{p} = \frac{h}{mv} \dots\dots\dots (1-1)$$

Where;

λ is the wavelength,

p is the momentum.

h is the Planck constant.

m is the mass.

v is the frequency.

When the confining dimension is large as it is in bulk, the particle behaves as if it were free compared to the wavelength of the particle. During this state, the bandgap remains at its original energy due to a continuous energy state. However, as the confining dimension decreases and reaches a certain limit, typically in nanoscale, the energy spectrum becomes discrete. As a result, the bandgap becomes size-dependent. This ultimately results in a blue shift in light emission as the size of the particles decreases (Cahay, 2001).

In metals and semiconductors, the electronic wave functions of conduction electrons are delocalized over the entire particle. Electrons can, therefore, be described as 'particles in a box', and the densities of state and the energies of the particles depend on the size of the box, which at first leads to a smooth size-dependence. However, when more atoms are added the shells are filled up and discontinuity occurs when a new shell at higher energy starts to be populated. Because of these discontinuities there is no simple scaling. Instead, one finds behavior akin to that of atoms, with filled shells of extra stability. Therefore, such clusters are often called 'pseudo-atoms'. The HOMO–LUMO band gap of semiconductor particles and, therefore, their absorption and fluorescence wavelengths become size dependent, Fig 1.1. Ionization potentials and electron affinities are tuned between the atomic values and the work function of the bulk material by variation of the cluster size. These same properties relate to the availability of electrons for forming bonds or getting involved

in redox reactions. Therefore, the catalytic activity and selectivity become functions of size (Roduner, 2006).

1.2.2.3 Antimicrobial activity

Some nanomaterials possess antiviral, antibacterial, and antifungal properties and have an excellent capability to deal with pathogen-related diseases. Hence, these features have made nanoscale materials valuable for a wide range of applications, substantially boosting the performances of various devices and materials in a number of fields (Baig *et al*.,2021).

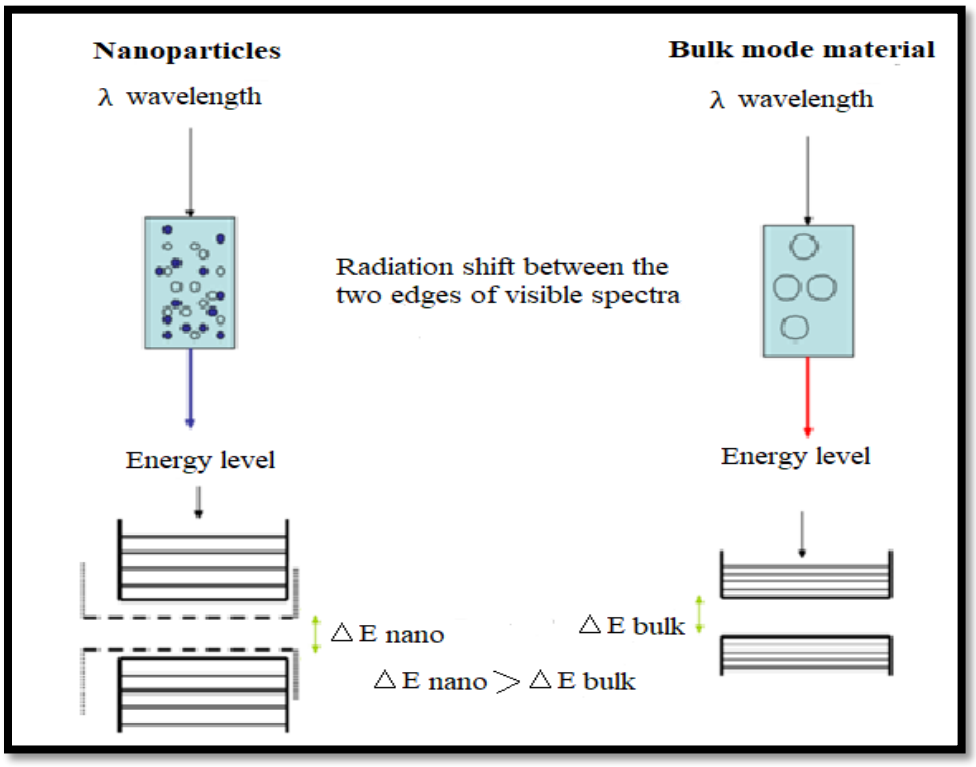

Fig.1.1 Radiation shift between the two edges of visible spectra (Nano and Bulk scales).

1.2.3 Nanomaterials preparation.

Increasing number of methods and techniques are developed to prepare and control the size and shape of nanoparticles. However, some of these methods have been

commercialized on a large scale, and many have yet to be scaled up to mass production.

In general, there are two approaches to prepare nanoparticles, top down and bottom up, top-down approach is used to produce structures with long-range order and for making macroscopic connections, while bottom-up approaches are best suited for assembly and establishing short-range order at nanoscale dimensions (Mendes *et al*., 2004).

1.2.3.1 Top down.

The top down approach Fig 1.2 works on the basis of breaking down and miniaturizing a large piece of material into a smaller piece, in this case with dimensions in the nanometer range (1-100 nm). The most common top-down approach of fabrication involves lithographic patterning, laser reduction technique, ball milling, electrospinning, sputtering …. etc. (Nguyen *et al*,2021; Hernández *et al.*,2021; Baig *et al*., 2021).

1.2.3.2 Bottom up

The bottom up approach, Fig 1.2, relies on using small molecules to prepare nanoparticles. Preparation of nanoparticles by the bottom up approach relies on the principle of supersaturation (Zaizer and Lamer, 1948). Bottom-up, or self-assembly, approach of nanofabrication uses chemical or physical forces operating at the nanoscale to assemble basic units into larger structures in simple terms, some techniques used in bottom up process such as chemical vapor deposition (CVD), solvothermal and hydrothermal methods, the sol–gel method, soft and hard templating methods, reverse micelle methods … etc. (Baig *et al*., 2021).

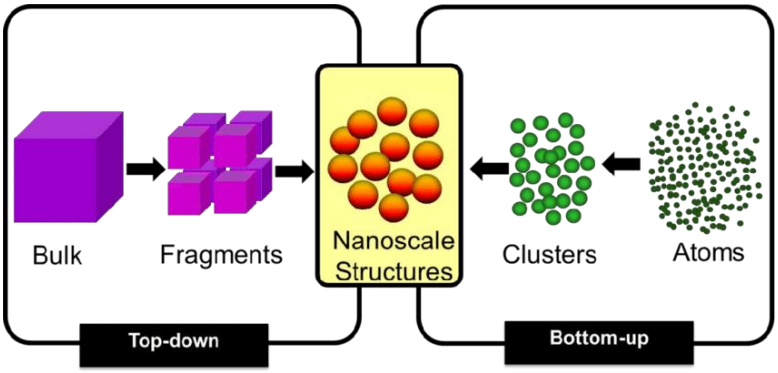

Fig. 1.2 "Top-down" and "Bottom-up" synthesis of nanoparticles.

1.2.4 Nanomaterials catalysis (Nanocatalysts).

Catalysis involves changing the rate of a chemical reaction, usually a speeding up or acceleration of the reaction rate, by the addition of a substance, called a catalyst that is not consumed during the reaction.

A catalytic agent (catalyst) is a material, typically a metal or alloy that enhances the rate of a chemicals reaction. There are two main types of catalysts, Homogeneous catalysts; are dispersed in the same phase as the reactants, the dispersal, ordinarily, being in a gas or a liquid phases. Heterogeneous catalysts; are in a different phase than the reactants, separated from them by a phase boundary. Heterogeneous catalytic reactions usually take place on the surface of a solid catalyst, such as silica or alumina, which has a very high surface area that typically arises from their porous or sponge like structure (Wang., 2017).

Catalysis is significant due to the unique capabilities of catalysts in accelerating chemical reactions by reducing the energy barrier (i.e., activation energy) of their transition states and in controlling reaction pathways toward selective synthesis of target products. Catalysts can be homogeneous or heterogeneous, depending on whether they exist in the same phase as the substrates or not. Because homogeneous catalysts are readily soluble and accessible to the substrates in reaction media, they possess high catalytic activity and selectivity under mild conditions. Moreover, their structures are well defined at the molecular level. These features render these

molecular catalysts capable of rationally tuning their catalytic properties by modification of their ligands and metals and tuning the reaction pathways. However, homogeneous catalysts are employed due to their ease separation and recovery, as well as their high stability even, when exposed to harsh reaction conditions. However, heterogeneous catalysts, usually, exhibit lower activity than their homogeneous counterparts, mainly, due to diffusion limits and the reduced number of active sites that are accessible to reactants. To overcome these limitations, which are associated with homogeneous and heterogeneous catalysts, new catalytic systems need to combine their advantages with respect to high efficiency, selectivity, stability, and preparability. Nanocatalysts are examples of this new catalytic system, which links homogeneous and heterogeneous catalysis. They are composed of nanosized particles (nanometals or nanometal oxides that are self-supported or dispersed on other surfaces) with a large exposed surface area of active components, which enhances the accessibility of their active sites to reactants and mimics homogeneous catalysts. Their insolubility in reaction solvents and reactants renders them easily separable from reaction mixtures, which enables their resemblance of heterogeneous catalysts. The activity and selectivity of nanocatalysts can be rationally, tuned by changing their chemical and physical properties, such as size, shape, composition, and morphology (Wang., 2017).

Since the end of the 1990s and with the development of nanoscience, nanocatalysis has emerged as a domain at the interface between homogeneous catalysis and heterogeneous catalysis. The main focus is the synthesis, characterization, exploration, and exploitation of, well-defined, nanostructured catalysts, which include nanoparticles (NPs) and nanomaterials (Wang., 2017).

1.2.4.1 Properties and structure–reactivity relationship of Nanocatalyst

Nanomaterials that, preferentially, expose the reactive crystallographic facets via size and shape control provide the possibility of finely tuning catalytically active

sites. The structure−reactivity relationship of metal catalysts has been, conventionally and qualitatively, interpreted in terms of electronic and geometric properties, caused by the size, morphology effects, chemical composition and high surface-to-volume ratio.

1.2.4.2 Size effect

Nanocatalysts are characterized by their unique nanoscale properties, which originate from the highly reduced dimensions of their, catalytically, active domains. The effect of particle size in the context of nanocatalyst has been well understood. The, lowly, coordinated atoms that are located in defects in solid catalyst particles, such as terraces, edges, kinks, and vacancies, have been considered to be active sites. By reducing the domain size of catalyst particle as far as possible, the number of active sites can be maximized. The effect of particle size is, frequently, employed to describe the relationship between the reaction and the catalyst particle size, especially in the size range 1 to 100 nm (Wang., 2017).

1.2.4.3 Morphology effect

Because heterogeneous catalysis, intrinsically, involves the cleavage and formation of chemical bonds between reactants and products at the surface of catalyst, these elementary steps can be, reasonably, assumed to be intimately, associated with the coordination environment of surface or active atoms. This dependence can be attributed to the exposed crystal facets that are, predominantly, determined by the shape of catalyst particle. Control of catalyst particle morphology enables a selective exposure of a larger fraction of the reactive facets on which the active sites can be enriched or tuned (Wang., 2017).

1.2.4.4 Composition effect

The need for promoters or multi-metallic catalytic systems has emerged due to several factors, including a reduction in the price of active catalysts and an increase in their activity, selectivity and long-term stability. As an example, bimetallic NPs

with core–shells, heterostructures, or intermetallic and alloyed structures are emerging as a new class of nanocatalysts. They are expected to display not only a combination of properties that are associated with two distinct metals but also new properties due to a synergy between the two metals (Wang., 2017).

1.2.4.5 Surface-to-volume ratio

Nanocrystals of finer sizes provide an increase in surface-to-volume ratios (A/V), which causes higher catalytic activity compared with large crystals of the same mass on surface and higher chemical reactivity. If N_t denotes the total number of atoms in a particle and N_s represents the number of atoms that reside on its surface, the higher N_s/N_t ratio is an important factor for catalytic performance of particle due to its higher A/V ratio (Wang., 2017).

The calculated surface/volume ratio for a thickness per shell is shown in Fig.1.3. By decreasing the particle size, the number of atoms on the surface or the *N*s/*N*t ratio is increased, that is, in the regime of fewer than 10 layers, which corresponds to ~3 nm (Burda *et al*., 2005).

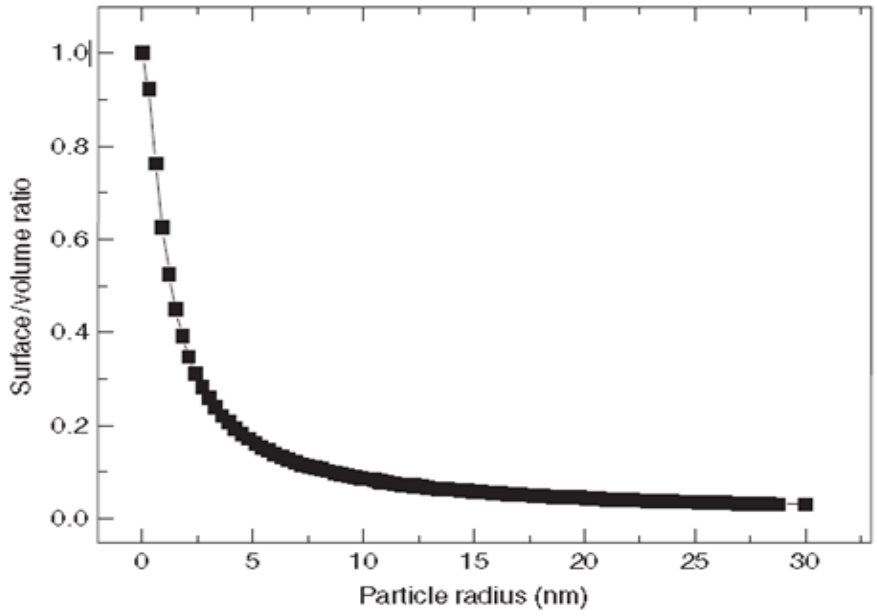

Fig. 1.3 Variation of *N*s/*N*t ratio with particle size.

1.3 Enhanced oil recovery (EOR)

In 2014 British Petroleum (B9410.P) reported, in its annual "Statistical Review of World Energy", that global oil consumption increased by 1.4 % above average equivalent to 1.4 million barrels per day (Petroleum B., 2014). Recently, High quality crude oil supply has drastically decreased which led to a shift toward abundant natural resources. Fig.1.4 shows that heavy oil and bitumen accounts for about 70 % of total remaining hydrocarbon resources (Alboudwarej *et al*., 2006).

The main characteristic of heavy oil is its density (weight per volume) or specific gravity that is commonly defined to be less than 20° American Petroleum Institute (API), and that due to the presence of high molecular weight compounds (Dusseault , 2001). Therefore, heavy oil with high viscosity has very poor flow rate and hence is very difficult to transport due to high internal resistance forces of high molecular weight molecules. Also, and due to presence of considerable amounts of

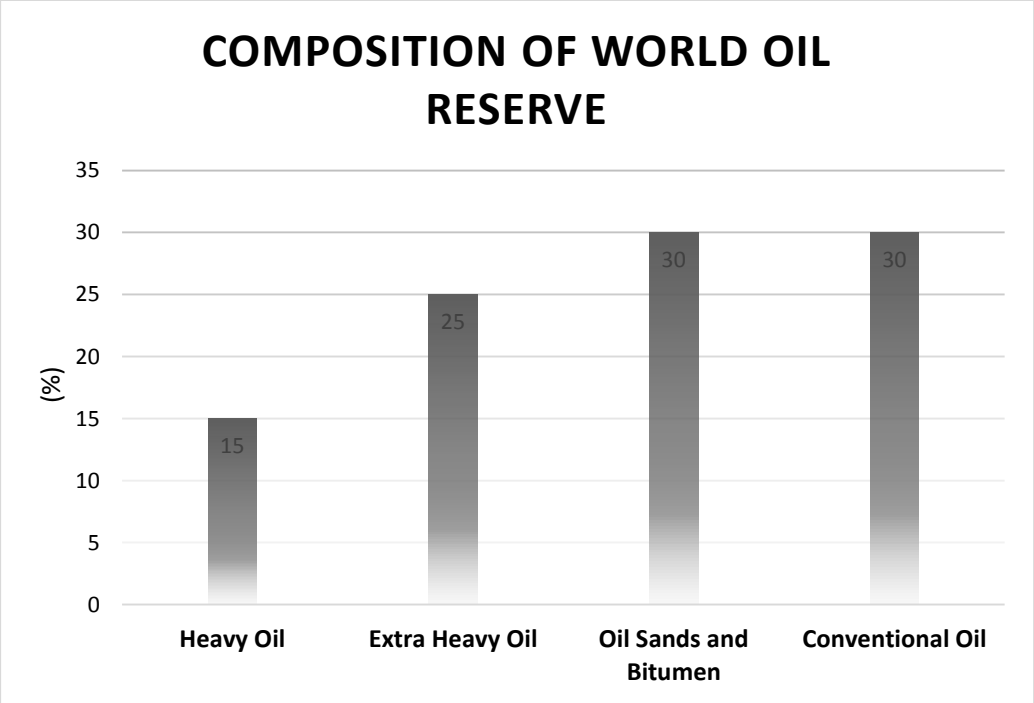

Fig. 1.4 column chart of total world oil reserves where unconventional hydrocarbon resources hold 70 % of the total reserves.

asphaltene and resin, heavy crude oil has a poor quality. Both of them, aspheltene and resin, have a high average molecular weight, and these, consequently, result in high production cost and difficulties in exploitation.

On the other hand, saturated and aromatic hydrocarbon are, generally, found in very low contents in heavy crude oil. The other constituent of unconventional oil is known as extra heavy oil, its main characteristics are low API (below 10°) and a viscosity of greater than 100 Pa.s by the World Energy Concil in 2010, however, its contribution to total world oil reserves is around 25 % (Iskandar *et al*,2016).

Several reaction methods have been developed and adopted in order to enhance heavy crude oil recovery and reduce its viscosity. Recently, a variety of methods exist and widely used for example, chemical flooding, water flooding, gas lifting for non-thermal treatment, steam injection for thermal treatment, hot water flooding and in-situ combustion for thermal treatment. These methods are the most popular and frequently used (Owen and Floyd, 1981). Hyne *et al* (1982) proposed another reaction, this reaction was called aquathermolysis, which is a promising way to noticeably reduce heavy oil viscosity noticeably, during this reaction, heavy oil will be added with water or steam at 200-280 °C and the time needed for the reaction to complete varied from a few hours up to several days.

Lately, it was noticed that aquathermolysis reaction solely using water hydrolysis did not proceed as well as it was predicted since the hetero atoms S, N and O in heavy oil molecule can interact with each other by means of hydrogen bonding or Van der Waals forces, and polymerize to form larger molecules. Therefore, this is not an effective way to reduce heavy oil viscosity (chen *et al*., 2008). Originally, most researchers used transition metal salts, transition metal compounds, and organometallic compounds in this technology, and later began to use solid super acids (Chen *et al*., 2016). Some researchers, intensively, studied the mechanism of catalytic aquathermolysis (Clark *et al*., 1984; Fan *et al*.,2006; He *et al*., 2006;

Shokrlu and Babadagli., 2014; Chen *et al*., 2016). They found that heteroatom (N, O and S), containing groups, in heavy oil could cause the polymerization, create the hydrogen bonds and finally lead to high viscosity. therefore, breaking heteroatom-containing groups would be a promising technique to reduce viscosity. Almost, all of researches supported the mechanism according to which the catalysts, mainly, catalyzed C–S bonds cleavage and that was the main reason why the viscosity of heavy oil was at last reduced. But later, it was found that besides C–S bonds cleavage, the catalyst, mainly, caused changes in oxygen containing groups, that is, the cleavage of C– O bonds in phenolic, ethereal molecules, etc. of the heavy oil (Chen *et al*., 2016). With the participation of transition metal ions (which attack heteroatoms of macromolecules in heavy oil), the C–R (R = S, N, O, etc.) bonds will be weakened and the superheated water interaction with these bonds could be successfully facilitated. The above problem statement, the need for a better solution is vital to improve the reaction efficiency. Catalysis science was nominated as one of reaction acceleration technique to solve the problem. As an illustration, using either mineral, water-soluble, oil soluble or nanoparticles catalysts is proposed to have a meaningful effect to overcome heteroatoms problem. This is due to the fact that a catalyst only acts as an intermediary substance between the reactants and the products by lowering the activation energy of the reaction (Chen *et al*., 2016).

1.4 Literature review

1.4.1 Synthesis of nickel nanoparticles (NiNPs)

Nickel (Ni) is a chemical element with atomic number 28, which belongs to the first two transition metals, has a partially filled 3d, orbital electron band and is very important to chemical reaction, in particular when in the powder form, having a larger surface area. On the other hand, in ambient air environment, Nickel will slowly react with oxygen to form Nickel oxide compounds. Nickel is quite abundant

on earth, but it is rarely found in pristine condition. It has been proposed that Nickel-iron is one of the components that form the earth's core (Iskandar *et al*., 2016).

Nickel has two manifestations of nanoparticles: nickel metal (Ni) and nickel oxide (NiO). These two classes of nanoparticles possess magnetic properties, biocompatibility, catalytic activity, antimicrobial activity and sorption nature. Further, NiONPs is a semiconductor (band gap: 3.6 to 4.9 eV) with high chemical stability and electron transfer ability (Thema *et al*., 2016). Hence these nanoparticles are finding wide applications in diverse fields such as electronics, energy applications, biomedicines, sensors, waste water treatment and various organic syntheses based on reduction, hydrogenation, alkylation and investigations are also being made in using these nanoparticles as adsorbents in water remediation methods (Ravindhranath and Ramamoorty., 2017).

Literature reports the synthesis of NiNPs using microwave assisted synthesis (Lai *et al*., 2006, Xu *et al*., 2008; Eluri and Paul, 2012), micro-emulsion synthesis (Van *et al*., 2020), chemical reduction technique using suitable reducing agents like sodium borohydride (Liu *et al*., 2021), and hydrazine hydrate (Wu and Chen, 2003, Ádám *et al*.,2020; Wu *et al*., 2012; Sudhasree *et al*., 2014), reversed micelles method (Harish *et al*., 2011), thermal decomposition of nickel (II) acetylacetonate in alkylamines (Chen *et al*., 2007) , electro deposition and sol-gel methods (Jia *et al*., 2008).

The commonly used precursors are nickel chloride, nickel sulphate, nickel acetate, nickel nitrate, nickel carboxylate *etc*. and the reducing agents are sodium borohydride, sodium hydride, hydrazine hydrate, organic amine (oleyl amine), primary aliphatic amines (dodecylamine), sodium hypophosphite *etc.* and the capping agents are polyvinyl pyrrolidone (PVP), sodium dodecyl sulfate, cetyltrimethylammonium bromide (CTAB) and the organic solvents used are ether, unsaturated alkynes, ethylene glycol, diethylene glycol, triethylene glycol,

polyethylene glycol, hexane, cyclohexane and octane *etc* (Pandey and Manivannan, 2015). The reducing agents convert the nickel ions to nickel atoms and thus formed metal atoms are 'oozed out' from the aqueous or organic mother liquors in the atomic/molecular forms as they are insoluble. Then they start growing by aggregation called Ostwald ripening, and when they come to the nano-size, the capping agents have to arrest the further growth or otherwise, the particles pass through the colloidal stage and precipitate (Sun *et al.*, 2007, Pandian *et al.*, 2015).

NiNPs, easily oxidize, and to stabilize them in aqueous solutions, capping agents are used. Most of the conventional synthetic capping agents are toxic. Hence, researchers are looking towards plants whose bio-extracts contain compounds that can serve as reducing agents as well as capping agents such as; sugars, vitamins., polyphenols etc.

Chen *et al*. (2014), used the extracts of *Medicago sativa* (alfalfa) for the synthesis of NiNPs. The precursor used was $Ni(NO_3)_2$ and the reduction was carried out at room temperature and the obtained particles were freeze-dried for one day to obtain NiNPs. In another work, Vaseem *et al*. (2013), found that glucose served both as reducing and capping agent, when Nickel salt solution was treated with glucose and ammonia. The aldehyde group in the glucose causes the reduction of Ni^{2+} to Ni and in doing so, it is oxidized to carboxylate group. Thus obtained caroxylate groups and hydroxyl groups in the glucose, are bound to the surface of NiNPs and thereby, prevent the aggregation of Ni particles consequently the NiNPs are capped. Dutta and Dolui (2011), synthesized NiNPs using naturally occurring tanic acid as reducing and stabilizing agent simultaneously. Mariam *et al*. (2014) used leaves extract of *Azadirachta indica* for the synthesis of NiNPs. Abhijit Kar and Ajoy Kumar Ray (2014), reported the use of Hibiscus rosasinensis petals soaked in Nickel chloride solution to obtain NiNPs of 10 to 200 nm size. These particles were found

to have carbon on their surface which prevented the agglomeration and responsible for stability of particles.

Well dispersed NiNPs with uniform size were synthesized via a modified hydrazine reduction route without any surfactant introduced. Interestingly, Ethanol was used as solvent and played the complementary reducing role. Pure metallic NiNPs could be easily obtained when ethanol instead of water was used as solvent. The particle surface was much improved when ethanol was involved in the reduction process at high temperature. The resultant particles have smooth surface and uniform size of about 50 nm. Also, Lenggo *et al*. (2003), synthesized Nickel oxide via spray pyrolysis using several precursors, such as Nickel chloride, nitrate and formate. Ai *et al*. (2004). synthesized and studied NiNPs prepared via wet chemical method using ethylene glycol (EG) as solvent. In his work, ethylene glycol acted as agglomeration-preventing agent, with forming a protective layer around the NiNPs, therefore, a well dispersed NiNPs has been created.

NiONPs have been developed using gelatin instead EG as organic solvent (Meneses *et al*., 2007). Although very small particles sized (3.2 nm) were successfully synthesized, the ploydispersed characteristic of nanoparticles still persisted as a major problem until Li *et al*. (2007) found a better way to synthesize NiNPs using the micro emulsion method. In micro emulsion technique, oil phase (e.g. cyclohexane, methyl cyclohexane) was used to prepare NiNPs nanocatalyst that could act as hydrogen donor to further improve heavy oil. Obtained NiNPs had a spherical shape and average diameter of 6.3 nm.

In a similar study, the hydrazine reduction method was applied for the synthesis of NiNPs without using inert atmosphere and added surface active agents, the obtained crystallite sizes could be tailored between 7 nm and 15 nm; however, the results revealed significant agglomeration resulting in aggregates with spherical or $Ni(OH)_2$ resembling morphologies depending on the solvent used. The catalytic activities of

the nanoparticles prepared were tested and compared in a Suzuki-Miyaura cross-coupling reaction (Ádám *et al*., 2019).

Wu and Montero *et al* (2010), synthesized pure spherical metallic NiNPs, by hydrazine reduction of Nickel chloride at room temperature without any protective agent and inert gas protection. This synthetic method is proven to be simple and very facile. In addition, it is very interesting to note that NiNPs can be isolated in stable solid state for several months in the atmosphere. The suggested mechanism for the NiNPs formation, as follows;

$$Ni^{+2} + 6C_2H_5OH \rightarrow [Ni(C_2H_5OH_6)]^{2+} \ldots\ldots\ldots\ldots\ldots\ldots\ldots\ldots\ldots\ldots\ldots\ldots\ldots\ldots (1\text{-}2)$$

$$[Ni(C_2H_5OH_6)]^{2+} + mN_2H_4 \rightarrow 6C_2H_5OH + [Ni(N_2H_4)_m]^{2+} \ldots\ldots\ldots (1\text{-}3)$$

$$[Ni(N_2H_4)_m]^{2+} + 2OH^- \rightarrow Ni(OH)_2 + mN_2H_4 \ldots\ldots\ldots\ldots\ldots\ldots\ldots\ldots\ldots (1\text{-}4)$$

$$Ni(OH)_2 + N_2H_4 \rightarrow Ni + N_2 + 2H_2O \ldots\ldots\ldots\ldots\ldots\ldots\ldots\ldots\ldots\ldots (1\text{-}5)$$

In a similar study by Elrbi and Paul (2012), synthesized of NiNPs in a static microchannel T-mixer by the reduction of $NiCl_2 \cdot 6H_2O$ in the presence of ethylene glycol without a stabilizing/capping agent. In their study, Nanoparticles were formed in accordance with the modified polyol process with hydrazine used as a reducing agent and NaOH as a catalyst for nanoparticle formation. Adaptation of this chemistry to a static microchannel T-mixer for continuous synthesis resulted in smooth, spherical particles. Under a reaction temperature of 130 °C resulted in a narrow size distribution of 5.3 ± 1 nm and also resulted in magnetic properties of 5.1 emu/g (saturation magnetization), 1.1 emu/g (remanent magnetization), and 62 O_e (coercivity).

Zhang *et al*. (2015), synthesized NiNPs of 10–30 nm in size by Ni^{2+} reduction using $NaBH_4$ at room temperature. The magnetic hysteresis measurement indicated that the NiNPs presented ferromagnetic properties, And the experimental results showed the as-obtained NiNPs might be a potential adsorbent in sewage treatment process.

Pandey and Manivannan (2015) synthesized NiNPs using hydrazine hydrate. The precursor used was Nickel chloride hexahydrate. Typical procedure for hydrazine hydrate reduction route involves dissolving the precursor salt in ethylene glycol, followed by the addition of hydrazine hydrate and NaOH to the reaction mixture. The purpose of the sodium hydroxide in the synthesis is to maintain medium alkalinity, ethylene glycol was used as a solvent. The black particles were washed using ethanol and dried in for 3 h oven at 80 °C. it has been found that Particles were found to be in amorphous form for the particles synthesized using molar ratio of 5:1, while for other two molar ratios, particles were found to be crystalline. Crystallinity increases with an increase in the molar ratio. Crystal size of the particles decreased with increase in the molar ratio of reducing agent to precursor. An optimum concentration of reducing agent to precursor is highly essential for the formation of the particles.

The standard reduction potential of hydrazine is respectively −1.16 in an alkaline solution, represented by the oxidation reaction when mixed with the nickel ions V (vs. SHE).

$$N_2H_4 + 4OH^- \rightarrow N_2 + 4H_2O + 4e^- \quad E^\circ = -1.16 \ldots\ldots\ldots \text{(1-6)}$$

Nickel, which has a standard reduction potential of −0.25V, is consequently able to be reduced by hydrazine (Goia, 2004; Park *et al*., 2006).

$$2Ni^{+2} + 4e^- \rightarrow 2Ni \quad E^\circ = -0.25V \ldots\ldots\ldots \text{(1-7)}$$

Therefore, a chemical reduction process of the Nickel ion with hydrazine as a reductant in an alkaline aqueous solution can be simply shown in the following equation:

$$2Ni^{+2} + N_2H_4 + 4OH^- \rightarrow 2Ni + N_2 + 4H_2O \ldots\ldots\ldots\ldots\text{(1-8)}$$

Also, Solution pH influences the synthesis of the nickel nanoparticles as seen in the Nernst equation (8).

$$E = E^0 - \frac{RT}{4F} ln \frac{1}{[OH^-]^4 [Ni^{2+}]^2} \quad \text{..... (1-9)}$$

$$E = E^0 - \frac{2.303}{4\,F} \log\{[OH^-]^4 [Ni^{2+}]^2\} \text{..... (1-10)}$$

The formation of the NiNPs was enhanced when the redox potential, the driving force of the reaction, increased due to the increase of the pH solution, by adding a strong base such as sodium hydroxide at a certain temperature and constant nickel ion concentration (Wu and Chen, 2003; Wang, *et al*., 2008; Tientong *et al*.,2014). Therefore, to prevent hydroxide precipitation, it is very important to keep the reduction process at a high pH, because the standard reduction potential of $Ni(OH)_2$ is −0.72 V (Tientong *et al*.,2014).

$$Ni(OH)_2 + 2e^- \rightarrow Ni + 2OH^- \quad E^0 = -0.72 \text{ V} \text{ ..... (1-11)}$$

1.4.2 Nickel nanoparicles (NiNPs) nanocatalyst

The oil and gas industry encounters technical challenges in the short future, due to quick diminish of resources. Moreover, exploration expenses will continue to increase. Meanwhile, global energy consumption is constantly increasing, the industry urgently needs technological innovations to meet this immediate demand. minor success has been achieved in solving these problems using conventional macro and micro materials. Nanotechnology is an area subject that has had a revolutionary impact on many aspects from medical applications to electronics, as with these fields, the oil and gas industry is expected to experience such progress (Zhe *et al*., 2018).

Heavy crude oil with high viscosity causes low primary production from heavy oil reservoirs. Among all recovery techniques that are used, thermal recovery method is the best for increasing production by decreasing heavy oil viscosity and increases its mobility; as a result, increase heavy oil recovery (Lashanizadegan *et al*, 2008). Nonetheless, the yield of thermal recovery is considered low. Oil viscosity and

relative permeability are the two main factors that control heavy oil mobility. Nanofluids have been found to have an inhibition effect on the asphaltene deposition, which prevents the blockage of oil flow and enables effective oil mobility (Franco, 2016)

Many recovery methods have been developed to extract heavy oil from their reservoirs. The underground refineries approach using nanocatalysts is one of the latest promising technique that can be an alternative to surface upgrading. It has been reported that the reduction of heavy oil viscosity is not only a high temperature effect but also from a series of chemical reactions. Metal and metal oxide NPs have unique properties compared to their macroscopic counterparts. These NPs were used as potential adsorbents and catalysts for heavy oil recovery (Alomair, 2015).

Shokrlu *et al*. (2013). used Fourier Transform Infrared Spectroscopy (TGA–FTIR) system to study the kinetics of heavy oil combustion at low temperatures, as well as the effect of a nickel ionic solution on this process, FTIR was used to analyze evolved gases, analysis revealed production of different oxygenated compounds, such as phenols, carboxylic acids, sulfones and side products such as sulfur dioxide. According to this analysis, using nickel ions decreased the concentration of oxygenated compounds in the evolved gases, and increased the concentration of carbon dioxide and water. It also decreased the concentration of sulfur dioxide. This effect was more promising at higher temperatures. This effect of nickel ions can be of great interest in improving the efficiency of the in situ combustion technique used for heavy-oil recovery.

Heavy oil reservoirs are the most well-known unconventional resources of energy. High viscosity of oil complicates the recovery, therefore, upgrading the oil during its recovery is a critical but challenging process. The existence of hetero-atoms such as sulfur, oxygen and nitrogen as well as metals such as nickel, vanadium iron and copper complicates the upgrading process further by bringing about more difficulties

to upgrading of heavy oil, their components usually exist in the asphaltene fraction of the heavy oil. However, asphaltenes play a crucial role in determination of the physical properties of Heavy crude oil and has a negative effect in the processing and refining crude oil. In fact, the highly viscous nature of heavy oil is a result of the presence of asphaltenes. The strong attractive forces among ashphaltenes molecules cause an unfavorable increase in the viscosity of heavy oil (Hamedi and Babadagli., 2014)

Thermal recovery methods and techniques become uneconomical and environmentally unfavorable because the high steam requirement in certain cases. On the other hand, recovered heavy oil has very low mobility, which makes the transportation is problematic and very costly. The viscosity of the produced products is lowered by the addition of proper diluents, C_{5+} paraffinic liquid hydrocarbon or condensate, to increase the mobility of transportation. dilution of the heavy oil can cause asphaltenes precipitation problems in the pipelines. Improving and developing thermal techniques can help to overcome aforementioned problems. Many investigation has been made to tackle these challenges (Clark *et al*., 1990; fan *et al*; 2004; Li *et al*. 2007; Hamedi-Shokrlu and Babadagli 2010, 2013 and 2014) and in situ combustion (Ramirez –Garnica *et al*. 2008; Hamedi-Shokrlu *et al*. 2013).

Calrk *et al*. (1990), reported the catalysis effect of a series of transition metal species, in ionic solution form, on the catalysis of aquathermolysis reaction. Aquathermolysis reaction refer to the chemical reactions occurring between heavy oil, water, and reservoir matrix at the steam-stimulation condition. Clark *et al*. (1990), reported that transition metal species resulted in the partial upgrading of the heavy oil and bitumen. Also, Fan *et al*. (2004), reported that the minerals can catalyze the aquathermolysis reaction and result in in-situ upgrading. Li *et al*. (2007), studied the effect of nickel catalysts, in particles form, on the upgrading of heavy oil during aquathermolysis. Hamedi-Shokrlu and Babadagli (2013) proposed the application of

nickel nanoparticles to overcome the mentioned problems to some extent. The approved that the nickel catalysts catalyze the breakage of C-S bonds in asphaltenes reaction in the heavy oil, which regenerated hydrogen sulfide and lighter hydrocarbon components, and the maximum upgrading was achieved with 500 ppm of NiNPs. Later, Hamedi-Shokrlu and Babadagli (2014), studied the interaction of the NiNPs with water, oil, and matrix by analyzing the electrostatic interactions between these media. They showed that one slug of a cationic surfactant must be injected into a silica based porous medium (sandstone) to alter the electric charges of the medium to positive. Then, the NiNPs can be introduced as stabilized with 300ppm of xanthan-gum polymer. With this technique, the particles move the oil in water interface and to surface of the matrix.

Hamed-Shokrlu and Babadagli *et al*. (2014), revealed that the NiNPs catalyzed the aquathermolysis process of steam stimulation. In their work, they studied the kinetics of NiNPs in this process. NiNPs were capable of reducing the activation energy of the main aquathermolysis reaction. The principle is that NiNPs break the C-S bonds in the compounds, reducing their molecular chain. Through this method, the concentration of the components with the carbon chain length, which was more than 31, was decreased resulting in the reduction in oil viscosity. Therefore, the energy usage was more efficient, and the heavy oil recovery is significantly increased.

Another investigation conducted by Zabala *et al*. (2016) revealed that the use of oil-based nanofluids (OBNs) reduced the oil viscosity at static conditions by approximately 98% without continuous injection. Hashemi *et al*. (2013) used Water-in-vacuum gas oil microemulsions containing trimetallic (W, Ni, and Mo) ultradispersed colloidal nanoparticles and conducted series of experiments at a pressure of 3.5 MPa, residence time of 36 h, and temperatures from 320 to 340 °C in an oil sands packed bed column of three consecutive categories of hot fluid

injection (in the presence or absence of trimetallic nanoparticles). For the first category, the obtained experimental results showed that the recovery curve for vacuum gas oil injection without nanocatalysts was at a plateau. In the second series of tests, observations proved that adding a certain percentage of pentane enhanced the recovery performance of injection tests. The third phase of experiments was conducted in the presence of trimetallic nanocatalysts in emulsion with vacuum gas oil. Their results showed the effectiveness of nanocatalysts for enhancing the recovery performance.

Li *et al.* (2007) applied NiNPs as catalyst in an aquathermolysis reaction of Liaohe extra heavy oil. It was observed that NiNPs catalyze aquathermolysis reaction of extra-heavy oil at 280 °C. As predicted, the best viscosity reduction of heavy oil as measured at 50 °C, this work was achieved with NiNPs. And the viscosity reduction was up to 98 %. Apart from viscosity reduction, H/C ration of crude oil was increased and a noticeable reduction of asphaltenes, resins and sulfur contents were also achieved in aquathermolysis reaction of heavy oil. Another attempt was conducted to prepare NiNPs through microemulsion technique by Wu *et al*. (2010), in his case, aquathermolysis reaction was done under much lower reaction temperature of 200 °C.

Chen *et al*. (2010) used GC/MS assisted with elemental analysis to compare the organic compounds in oil, water and gas phases before and after the aquathermolysis reaction, they found that a new kind of catalyst aromatic sulfonic ($H_3PMo_{12}O_{40}$) can reduce the viscosity of heavy oil through catalytic aquathermolysis, and results indicated that the catalyst could not only break the C-C bond, but also rupture the C-O bond in the heavy compounds.

In another study by Chen *et al*. (2016) a series of transition metal-Mannich base complex was synthesized and screened for catalytic aquathermolysis of heavy oil, the results showed that the Ni(II)-Mannich base complex is the most effective one.

It has been reported that, the viscosity of the heavy oil can be decreased by 82.6% using 1.0 wt % catalyst with 15 wt % methanol in a reaction at 180 **C** for 24 h, and the composition analysis shows that 9.0% asphaltene is converted to resin and saturated hydrocarbons.

Clark and Hyne (1984) analyzed the produced gases during the steam stimulation of heavy oil, and concluded that steam–oil interactions are chemical as well as physical. These chemical reactions occur among high temperature and pressure water, oil, and sand, and improve the physical properties of heavy oil/bitumen after steam stimulation, also they stated that hydrolysis of sulfur bridge of organosulfur compounds in heavy oil/bitumen is the important step of aquathermolysis. Hydrolysis is achieved by transferring hydrogen from water to the oil via water gas shift reaction (WGSR).

$$CO + H_2O \rightarrow CO_2 + H_2 \ldots\ldots (1\text{-}12)$$

The hydrolysis resulted in cleavage of S–C bonds, and releases H_2S gas. The WGSR is catalyzed by a variety of compounds, e.g. iron oxide, therefore, water is the main phase of the aquathermolysis process. Hascakir *et al*. (2008) reduced heavy oil viscosity without adding water at ambient condition. In their study, micron sized metal particles were mixed with different oil samples. After addition of the optimum concentration of particles to the sample, the yield point and its resistance to flow decreased. Thus, viscosity of the sample was decreased significantly after a short time. The well-known rusting reaction of iron is one example of such reactions. About 30% of viscosity reduction was achieved at temperature (80 °C) (Shokrlu, and Babadagli, 2014). Clark *et al*. (1990) reported a similar trend of viscosity reduction with aqueous metal salts after steam stimulation. Hamedi Shokrlu *et al.* (2013) studied the effect of nickel ions on heavy oil combustion, and they found that Nickel ions decreased the activation energy of the process from 16.9 kJ/mol to 10.9 kJ/mol. Elshawaf (2018) achieved 20-60 % viscosity reduction using graphene oxide

nanoparticles at temperature range from 40 to 100 °C. Shaban *et al*. (2014) reported that the viscosity reduction was 78.6 % by treating the heavy crude oil with imidazolium tetracholoferrate [BMIM][$FeCl_4$] at 90 °C. In another study by Chen *et al*. (2016) the viscosity of the heavy oil can be decreased by 82.6% using 1.0 wt % catalyst (Ni(II)-Mannich base complex) with 15 wt % methanol in a reaction under 180 °C for 24 h. Montes *et al*. (2020) reported 30% of heavy crude oil viscosity reduction with 1000 mg L^{-1} using silica nanoparticles. Sodium cloisite Na^+ nanoparticle alone was able to lower the viscosity of crude oil to about 92.5%, Poly (ethylene-co-vinyl acetate) (EVA) and Poly (maleic anhydride-alt-1-octadecene) (MA) were able to reduce the viscosity up to 88% and 86.4%, respectively while EVA and MA added to nanoparticle was able to reduce the viscosity up to about 94% and 89.2% (Subramanie *et al*.,2020).

1.4.3 NiNPs in water treatment

NiNPs or NiONPs are less investigated in the treatment of waste waters, in contrast to the large literature available pertaining to their applications in other fields of research, catalytic, anti-microbial, bio-medical, Electrochemical, sensor etc.

During crude oil recovery processes, plenty of water is produced together with the crude oil, as much as 20 times of oil, and treating this contaminated water for safe disposal or re-usage, is a very complicated and expensive process. The biggest challenge of the produced water treatment is the removal of dispersed oil. U.S Environmental Protection Agency (USEPA) requires a zero oil (0 mg L^{-1}) for discharging the produced water from the onshore production. While for offshore production, USEPA limits the discharge of oil and grease in produced water to maximum of 72 mg/L and a 30- day average of 48 mg/L (USEPA, 2004). However, nearly, 60 % of offshore platforms in Gulf of Mexico are believed not to be able to reach USEPA discharge requirement (Thoma *et al*.,1999). The convention for the Protection of Marine Environment of the North-East Atlantic (2005) further limits

the sea discharge of produced water to be 40 mg/L as a maximum concentration of dispersed oil. Many treatment technologies are recently developed to treat and remove the dispersed oil from produced water, such as gas flotation, coalesecers, gravity oil separation, hydrocyclones, memberane and corrugated plate interceptors. CPIs (Fakhru'l-Razi *et al.*, 2009). For offshore operations, and due to small space of platforms, a compact rapid treatment techniques are required. In this context, removal of dispersed oil from produced water, especially small oil droplets, are challenging because of the long residence times and hence large equipment volumes are typically essential. Therefore, there have been increasing attention and great efforts to establish a facile, low cost and efficient treatment technologies to treat produced water (Prigiobbe *et al*., 2014).

In recent years, the use of nanoparticles that can be synthesized in a controlled manner is attracting the researchers interest. And their applications are being developed and manipulated increasingly in many fields, i.e., pharmaceutical field uses the nanoparticles in drug delivery, DNA and cell tagging and separation in biology and medicine, information storage in electronics, environmental in green chemistry, catalysis and sensors (Prigiobbe *et al*., 2014). In petroleum industry, the use of nanoparticles is actively perused as a potential solution to many oilfield problems (Matteo *et al*., 2012).

The use of nanotechnology and nanoparticles for produced water treatment is a promising way to enhance de-oiling efficiency that current produced water treatment technologies face. The most attractive merit for nanoparticles, especially magnetic nanoparticles, is their quick response to move in a desire direction with application of external magnetic field. Also, magnetic forces can be orders of magnitude larger than gravitation, allowing much faster separation of the magnetic nanoparticles, small oil droplets from the dispersing water or oil medium. Magnetic nanoparticles adsorb the oil droplets, through the surface interactions between droplets and surface

of nanoparticles (Prigiobbe *et al*., 2014). Many researchers succeeded in developing various magnetic nanoparticles and manupliate their surfaces for a proper oilfield usage (e.g. Yoon *et al*., 2011; Yoon *et al*., 2012; Bagaria *et al*., 2013). Pen and co-wrokers (2012) demonstrated a good water removal capability from water-in- oil emulsions, they used in-house synthesized magnetic nanoparticles. Due to the ease of surface manipulation and modification, magnetic nanoparticles can be used for selective removal of a wide variety of compound for different water management purpose. On the other hand, one of the benefits that magnetic nanoparticles possess is the ability of regeneration the adsorbent for re-use purposes and increase the life time of their usage. Peng *et al*. (2012) were able to regenerate magnetic nanoparticles by using an organic solvent for washing the adorbate (chloroform- acetonitrile) and they used the regenerated their materials for ten times with good stability and their efficiency as well. Prigiobbe *et al*. (2014) performed batch scale experiments for oil droplet removal and 5 wt% decane from produced water using surface-coated magnetic nanoparticles, and their results showed that 85-99.99 % of decane can be removed, depending on the experiment conditions. Anionic surfactant-coated magnetic nanoparticles did not remove oil droplet, they attributed that for the electrostatic attraction between emulsion and magnetic nanoparticles which control the attachment of droplet on the surface. Also, they found that when a magnetic field is applied, velocity calculation of droplet settled spontaneously, and velocity of settlement strongly depends on the intensity of the applied magnetic field.

Mingyi Tang *et al*. (2014) used NiNPs prepared by $NaBH_4$ reduction and loaded poly (acrylamide-co-acryl acid) as a catalyst and studied the removal of potential organic pollutant (4-nitrophenol). Roya Nateghi *et al*. (2012) investigated the removal of mono azo Orange II dye from waste waters using commercially available nano NiO as adsorbent and found to be very effective. In another study, the surface of the adsorbent diatomite was modified with NiONPs and was used in the extraction

of basic red 46 (Khalighi *et al*., 2012). Under optimum extraction conditions, the adsorption capacity was found to be 105.61 mg/g (pH:7; temp. 25 ± 1 **C**, equilibration time: 1 hr.; 200 rpm; initial conc. of dye: 25 ppm).

Luo and co-workers (2016) fabricated superhydrophilic copper mesh decorated with nickel nanoparticles (Ni-NPs) via electrodeposition in fluorine-containing electrolyte. The size of NiNPs that consists of a metal Ni core and a polar $NiO/Ni(OH)_2$ shell was about 300 nm; moreover, the Ni-NPs combined with each other to form treelike nickel crystals by varying the experimental parameters. This optimized mesh exhibited remarkable oil in water separation performance. The oil content in separated water was lower than 3 mg L^{-1}, and the stability in acidic, alkaline, and salt solutions and the properties for repeated use are also excellent.

1.4.4 Adsorption isotherms (Langmuir and Freundlich)

Adsorption is usually described through isotherms, that is, functions which relate the amount of adsorbate on the adsorbent. Distribution of any adsorbate between the liquid phase and the solid phase can be described by several isotherm models such as Langmuir and Freundlich. The Langmuir isotherm assumes monolayer adsorption onto a surface containing a finite number of adsorption sites of uniform strategies with no transmigration of adsorbate in the plane surface (Desta, 2013). Once a site is filled, no further sorption can take place at that site. This indicates that the surface reaches a saturation point where the maximum adsorption of the surface will be achieved. The Langmuir isotherm is represented by eq. (1-13)

$$q_e = \frac{q_{max} K_L C_e}{1 + K_L C_e} \quad \text{..... (1-13)}$$

This isotherm was transformed into a linear isotherm, as it is presented in eq. (1-14).

$$\frac{1}{q_e} = \frac{1}{q_{max} K_L C_e} + \frac{1}{q_{max}} \quad \text{..... (1-14)}$$

Where;

q_e represents the adsorption capacity (mg g^{-1}).

C_e represent the equilibrium concentrations (mg L^{-1})

q_{max}represents the maximum adsorption capacity (mg g^{-1})

K_L (L mg^{-1}) is the Langmuir's isotherm constant which shows the binding affinity between dispersed oil and NiNPs.

(R_L) is the separation factor and it can be calculated using eq. (1-15).

$$R_L = \frac{1}{1+C_i \times K_L} \quad \text{..... (1-15)}$$

Where; R_L is the dimensionless Langmuir constant which indicate the adsorption possibility either favorable ($0 < R_L > 1$), unfavorable ($R_L > 1$), linear ($R_L = 1$) or irreversible ($R_L=0$) (Ayub *et al*., 2020).

Eq. (1-16) represents the Freundlich's isotherm.

$$q_e = K_f C_e^{\frac{1}{n}} \quad \text{..... (1-16)}$$

The linear form of Freundlich's isotherm is shown in eq. (1-17).

$$Log q_e = Log\ K_f + \frac{1}{n}\ Log\ C_e \text{..... (1-17)}$$

Where;

K_f is the Freundlich's constant (adsorption capacity).

1/n is the adsorption intensity.

The value of 1/n demonstrates the adsorption process either favorable ($0.1 < 1/n < 0.5$) or unfavorable ($1/n > 2$) (Ayub *et al*., 2020).

1.5 Objectives of the research

The aim of this study is to:

1. Synthesis and characterization of nickel nanoparticles(NiNPs) using hydrazine monohydarate as a reducing agent.
2. Investigate the effect of nickel nanoparticles (NiNPs) in heavy oil viscosity reduction.
3. Study the efficiency of nickel nanoparticels (NiNPS) in produced water treatment.

Chapter Two
Materials and Methods

Chapter Two

2. Materials and methods

2.1 Materials

2.1.1 Samples

Crude oil samples were randomly obtained from Baleela oilfield in West Kordofan state, Sudan. They were collected in a polypropylene plastic container. Produced water samples were also collected from the inlet valve of produced water tanks in a borosilicate glass tubes.

2.1.2 Chemicals

All chemicals used are of Analar grade except where stated.

2.2 Methods

2.2.1 Synthesis of Nickel nanoparticles (NiNPs)

(3.0) g of Nickel(II) chloride hexahydrate ($NiCl_2.6H_2O$) were dissolved in (25) mL absolute ethanol. (4.38) g of Solid sodium hydroxide (NaOH) were dissolved in (25) mL absolute ethanol, (5.4 and 8.2) g of hydrazine monohydrate ($N_2H_4.H_2O$) were added. Then, (N_2H_4/NaOH) mixture was added to $NiCl_2.6H_2O$ mixture, solutions were maintained at 60 °C with continuous stirring for 2 hours (ratio between Ni^{2+}/N_2H_4 was 10 and 15). The mixture turned blue (A), fig.1.5, and after 2 minutes it turned to grey (B) and finally to black (C), the obtained precipitate was collected on a 0.45 μ filter, washed by absolute ethanol, deionized water and acetone. The precipitate was dried in room temperature and stored in a capped container for further analysis.

($NiCl_2.6H_2O$) Mixture (A) Mixture (B) Mixture (C)

Fig. 1.5 Preparation of NiNPs.

2.2.1 Characterization of Nickel nanoparticles (NiNPs)

2.2.1.1 The X-ray diffraction (XRD)

The XRD analysis was performed using PANalytical 3 kW X'pert Powder XRD Multifunctional diffractometer with Cu Kα radiation source (λ=0.1594 nm). The XRD pattern were recorded for 2θ values in the range of 20°-120° with step size of 0.0262°. The samples were dried thoroughly before the analysis. To identify the reflections of the NPs, the JCPDS (Joint Committee of Powder Diffraction Standards) database was utilized. The average crystal sizes of the particles prepared were calculated from the full width at half maximum of the most intense reflection of metallic nickel applying the Scherrer equation. From the full width at half maximum, average grain size of the samples can be calculated. For the (111), (200), (220) diffraction peak, using Scherrer equation

$$d = \frac{K\lambda}{\beta}\cos\theta \quad \ldots\ldots (2\text{-}1)$$

Where;

d is the grain size;

K = 0.89 is the Scherrer constant related to the shape and index (h k l) of the crystal;

λ is the wavelength of the X-rays;

θ is the diffraction angle;

and β is the corrected full width at half maximum (in radians).

2.2.1.2: Transmission electron microscope (TEM)

A specimen for TEM detection was prepared by depositing a (5) μL microemulsion containing the metal nickel onto a gold grid coated with carbon. Then, the specimen was dried in a vacuum oven at 200 °C (in nitrogen atmosphere) for 24 h to remove water, organic solvent and surfactant. The size of catalyst particles in the treated

specimen was measured by an H700H type Transmission Electron Microscope (TEM).

2.2.1.3 Thermo-gravimetric and differential scanning calorimetry analysis (TGA- DSC).

Thermogravimetric analysis (TGA) combined with differential scanning calorimetry (DSC) is the preferred method to give valuable information on the thermal stability, activation energy and reactivity of the powders. The TGA and DSC analysis of NiNPs powder was uniformly placed in a Al_2O_3 crucible of (6.8) mm diameter and (85) µl volume. The test was conducted in nitrogen atmosphere on a NETZSCH STA449F3 thermal analyzer at a scanning rate of 10 °C/min.

2.2.1.4: Fourier transform infrared spectroscopy (FTIR).

(0.1) g of NiNPs was mixed with (1.0) g of KBr, spectroscopy grade (Sharlau), in a mortar. Part of this mix was introduced in a cell connected to a piston. The mix was converted to a solid disc which was placed in an oven at 105 °C for 4 hours to prevent any interference with any existing water vapor or carbon dioxide molecules, transferred to the FTIR analyzer (FTIR-84005 (SHIMADZU Corporation Kyoto, Japan), and a corresponding chromatogram was obtained showing the wave lengths of the different functional groups of the sample, identified by comparing these values with those in the library.

2.2.2: Applications of NiNPs.

2.2.2.1: Effect of NiNPs on crude oil rheology.

(0.05) g (0.05) % of NiNPs were added to (100) mL of crude oil. Then mixture was heated to 70 °C in a water bath for 24 h with continuous stirring. The mixture was cooled to about 50 °C, transferred a clean beaker and Δη (%) was calculated as follows;

$$\Delta\eta = \left[\left(\frac{\eta_0 - \eta}{\eta_0}\right) x\ 100\right] \text{.....(2-2)}$$

Where;

$\Delta\eta$ is the rate of viscosity reduction,

η^0 is the viscosity of the oil before the reaction.

and η is the viscosity of the oil and NiNPs mixture in mPa.s (Chen *et al*.,2016).

2.2.2.2 Determination of base sediment and water (BS&W) in crude oil (ASTM D 4007., 1995).

Two centrifuge tubes were filled to the 50-mL mark with sample. (50) mL of Varsol and (0.2) mL of demulsifier. The tubes were tightly closed and inverted ten times to ensure that the oil and solvent were uniformly mixed, then were immersed in water bath at 60 °C for 15 mins. Then, the tubes were centrifuged at (1500 rpm) for 10 min at 60 °C. Immediately after the centrifugation, water and sediment volumes were read and recorded.

2.2.2.3 Determination of API, density and relative density of crude oils (ASTM D 5002., 1996).

(0.7) mL of crude oil were injected in the density meter (Anton Paar DMA 5000., Germany). Density, specific gravity (SG) and American petroleum institute number (API) at 50 °C were measured.

2.2.2.4 Determination of dynamic viscosity by Brookfield DV-III

Test cell was filled with (13) mL of fresh crude oil, and temperature sensor was connected. A spindle No. 34 was attached to the instrument and immersed in the sample. Then, the rotate per min (rpm) was set to give an optimum recommended torque for the test (between 70 – 80 %).

2.2.2.5 Determination of adsorption capacity

Initial concentration (C_i) of dispersed oil in produced water sample was measured using (HACH DR 6000, USA), a series of different weights of the NiNPs ranging from (0.01), (0.02), (0.04) and (0.05) g were accurately weighed and added to 100 mL of produced water, the test tubes were gently shaken (at a constant rate), and

were placed in the water bath at 60 °C. The concentration of each sample was measured and the logarithm of (q_e) (the adsorption capacity mg g^{-1}) was plotted against the logarithm of the residual concentration (C_e), The adsorption capacity (q_e) and removal efficiency (%) at equilibrium were determined using Eqs. (2-3) and (2-4), respectively.

$$\text{The adsorption capacity } q_e = \frac{C_i - C_e}{W} \times V \quad \ldots\ldots\ldots\ldots\ldots\ldots \text{(2-3)}$$

$$\text{Removal efficiency \%} = \frac{C_i - C_e}{C_i} \times 100 \quad \ldots\ldots\ldots\ldots\ldots\ldots \text{(2-4)}$$

Where; q_e represents the adsorption capacity (mg g^{-1}).

C_i represent the initial concentration (mg L^{-1}).

C_e represent the equilibrium concentrations (mg L^{-1})

V is the solution volume (L).

W is mass (g) of the adsorbent (Ayub *et al.*, 2020).

Chapter Three

Results and Discussions

Chapter Three

3. Results and Discussions

3.1 Synthesis and characterization of NiNPs

3.1.1 Effect of temperature and (N_2H_4) / (Ni^{+2}) on NiNPs

Results of experiments conducted at room temperature, the reaction was not completed and no nickel was formed with both ratios. But, When the reaction temperature was raised to 60 °C, the instantaneous generation of black precipitates was observed, and the reaction was completed in less than 5 min, the yield was 90 %, similar results were obtained by many researchers (Wu *et al*., 2003; Bai *et al*., 2008; Khanna *et al*., 2009; Zhu *et al*., 2019).

3.1.2 The X-ray diffraction (XRD).

Fig.3.1(a) shows the XRD pattern of NiNPs prepared with a molar ratio of $N_2H_4/Ni^{2+}$was 10 and Fig.3.1 (b) when the molar ratio of $N_2H_4/Ni^{2+}$was 15, the XRD spectrum when the ratio was 10 display three distinct diffraction peaks at 44.57°, 51.9°, and 76.4°. The highest intensity for the peak observed was at 2θ value 44.57°. Their corresponding miller indices (111) and (200) confirm that the resulting powders were face-centered-cube (fcc) nickel. the XRD spectrum when the ratio was 15, displays three distinct diffraction peaks at 44.52°, 51.70°, and 76.39°. The highest intensity for the peak observed was at 2θ value 44.52°. Their corresponding miller indices (111) and (200) confirm that the resulting powders were face-centered cube (fcc) nickel. No other species were observed in the XRD pattern, indicating that pure nickel powders was formed. The XRD pattern matches that of the Joint Committee on Powder Diffraction Standards database (JCPDS PDF No.:04–0850) that confirms the random powdered arrangement for Nickel. Moreover, the average particle size determined using the Debye-Scherrer equation was found to be 12 nm for both ratios.

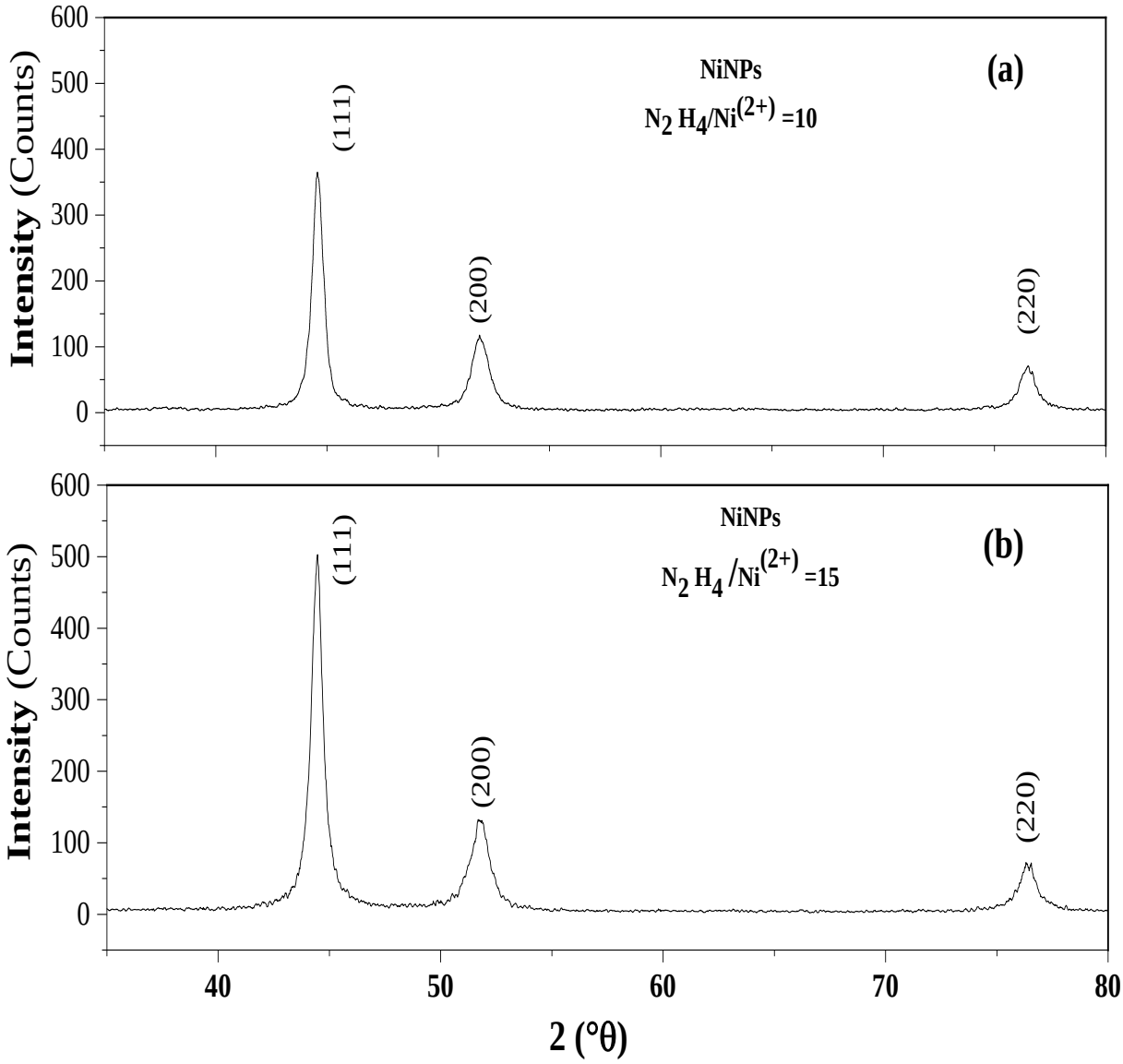

Fig. 3.1 XRD of NiNPs with the molar ratio(N_2H_4/Ni^{2+}) (a) 10:1 (b) 15:1

The X-ray diffraction results evidenced that the nickel nanoparticles formed by the reduction of Ni^{2+} with hydrazine were crystalline and this is in good agreement with the earlier reports (Wu *et al*.,2003; Bai *et al*., 2008; Khanna *et al*., 2009; Wu *et al*.,2012; Zhu *et al*., 2019; Ghanbarabadi and Khoshandam., 2020; Liu *et al*., 2021). Phase analysis by XRD revealed that no oxides or hydroxide such as NiO, Ni_2O_3, and $Ni(OH)_2$ were formed. This could be attributed to two facts: (i) the reaction was performed in an organic solvent instead of an aqueous solution, so it was relatively

easy to form pure nickel; (ii) it was observed that N_2 gas was produced and bubbled up continuously during the reaction according to equation (3-1);

$$2Ni^{+2} + N_2H_4 + 4OH^- \rightarrow 2Ni + N_2 + 4H_2O \quad \ldots\ldots\ldots\ldots (3\text{-}1)$$

which created an inert atmosphere and hence the input of extra N_2 gas was not necessary for the synthesis of pure NiNPs. Similar results were obtained by (Wu *et al*.,2003).

3.1.3 Transmission electron microscope (TEM)

A typical TEM micrograph and the size distribution for the NiNPs are shown in Fig.3.2 (a-d) when the molar ratio of $N_2H_4/Ni^{2+}$was 10 and Fig.3.3 (a-d) when the molar ratio of $N_2H_4/Ni^{2+}$was 15.

TEM images observed under low, medium, and high magnifications of the NiNPs, results when the molar ratio of $N_2H_4/Ni^{2+}$was 10 showed that the morphology is star-like with an average size 70-90 nm, similar results were obtained by Zhu *et al*. (2019), in their study, they used ethanol as a solvent and hydrazine as reductant but without a surfactant, however, the particles size was (2 μm) and with ununiformed morphology and thorny nickel nanowires or rose-like nickel crystals were obtained in the synthesis process. interestingly, very smaller particle size and uniformed morphology were obtained in our study without using a capping agent as can be seen in the TEM images in Fig.3.2 (a-d). Fig.3.3 (a-d) TEM images observed under low, medium, and high magnifications of the NiNPs when the molar ratio of $N_2H_4/Ni^{2+}$was 15, results show that the morphology changed to monodispersed spherical particles with an average size of 50-80 nm. It was found that, with increasing the ratio of N_2H_4/Ni^{2+}, the mean diameter decreased and the morphologies of NiNPs changed from star-like to spherical shape.

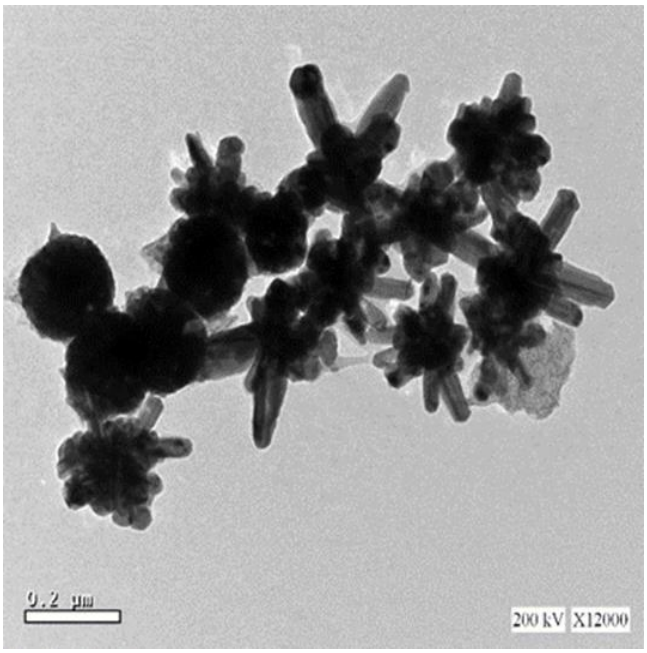

(a)

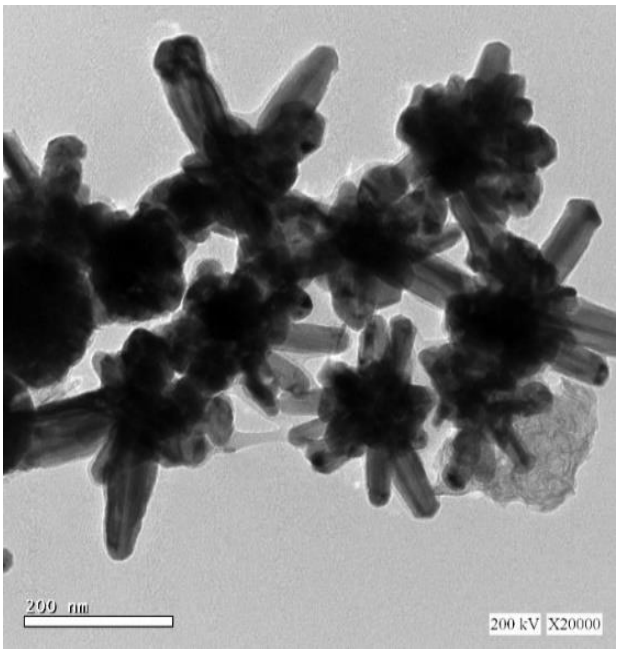

(b)

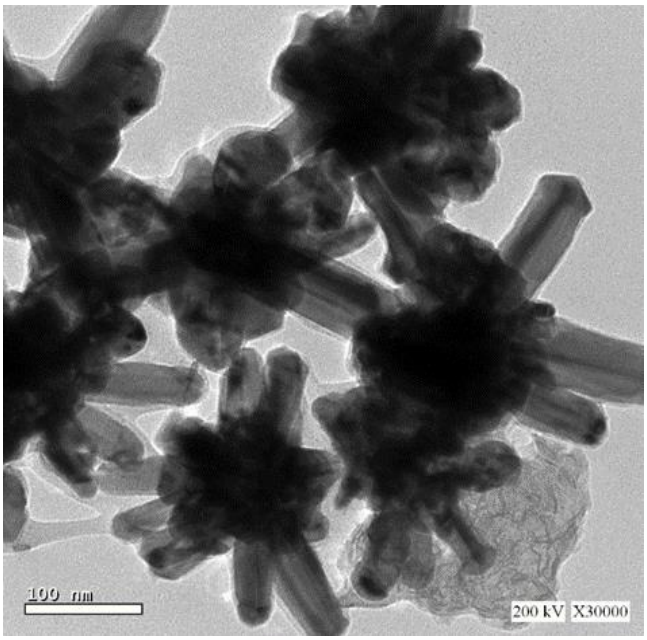

(c)

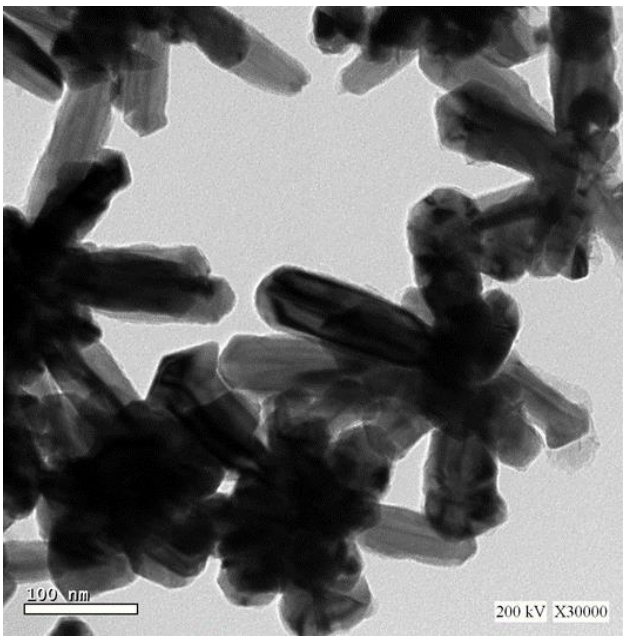

(d)

Fig.3.2 (a-d): TEM images of 10:1 (N_2H_4/Ni^{2+}) molar ratio, (a)0.2 µ(b)200 nm(c)100 nm(d)100nm

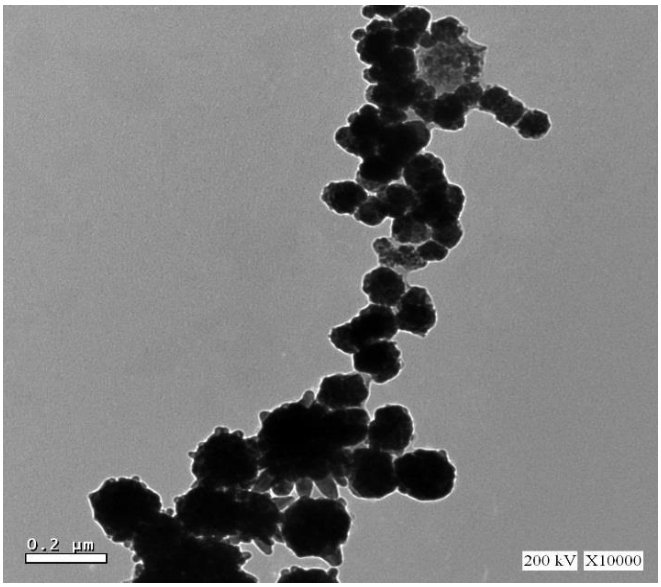

(a)

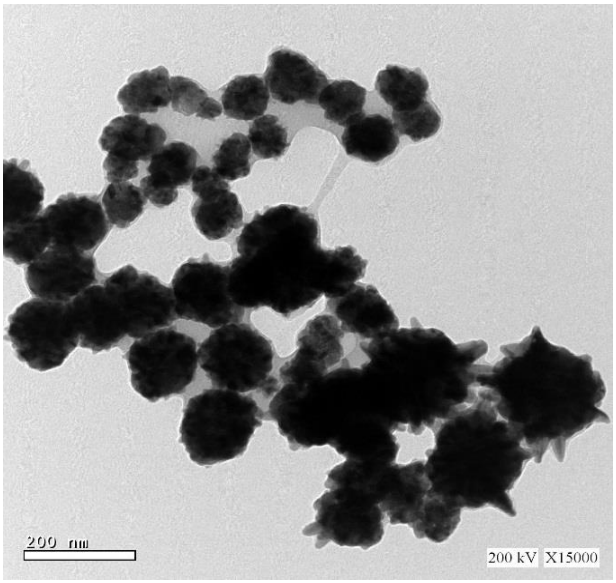

(b)

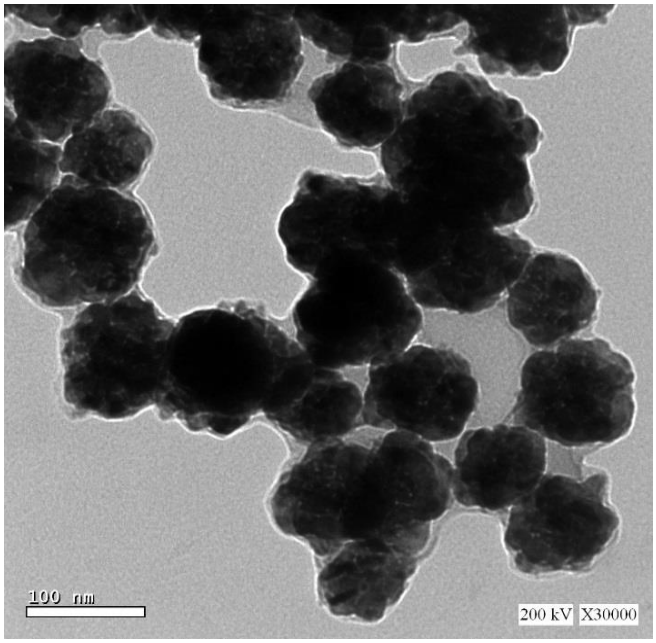

(c)

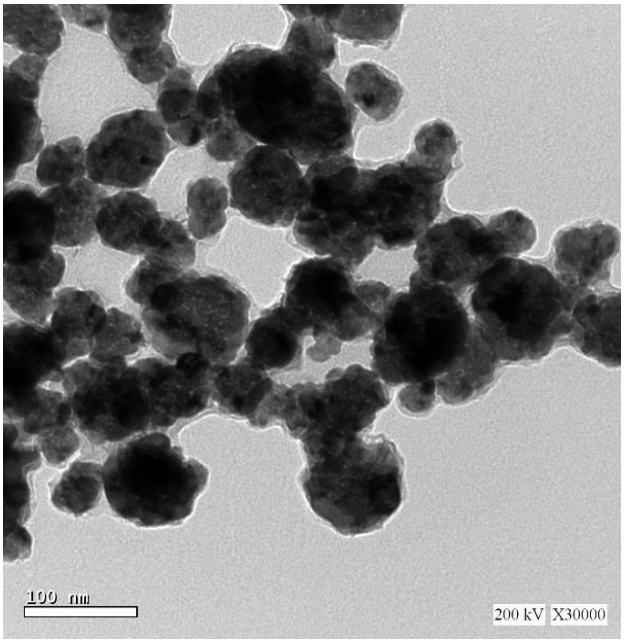

(d)

Fig.3.3 (a-d): TEM images of 15:1 N_2H_2/Ni^{2+} molar ratio, (a)0.2 µ(b)200 nm(c)100 nm(d)100nm

This phenomenon can be explained by the influence of the reduction rate on nucleation. It is known that a collision between several atoms must occur for nucleation since a minimum number of atoms is required to form a stable nucleus (Bai *et al*., 2008). However, the probability is much lower than the collision probability between one atom and a nucleus already formed. Once the nuclei are formed, the growth process will be faster than nucleation. moreover, when most nuclei are formed almost at the same time and grow at the same rate, the resultant nanoparticles will be monodispersed. Therefore, for the formation of monodispersed nanoparticles, the particle number and size are determined by the number of nuclei formed at the very beginning of the reduction. At a low hydrazine concentration (N_2H_4/Ni^{2+} = 10), the formation of larger particles with star-like shapes could be attributed to the fact that the reduction rate of nickel chloride was slow and only a few nuclei were formed at the beginning of the reduction reaction. Besides, the atoms formed at the beginning might participate mainly in collisions with already formed nuclei, instead of the formation of new nuclei. While, with the increase of hydrazine concentration, the reduction rate favored the generation of much more nuclei and the formation of smaller NiNPs. Additionally, at a high ratio, the reduction rate of nickel chloride was much faster than the nucleation rate and almost all nickel ions were reduced to atoms before the formation of nuclei, therefore, the nucleation rate was not further raised and the number of nuclei held constant with the increase of hydrazine concentration. Similar results were obtained by Wu and Chen (2003), their study was conducted in ethylene glycol as a solvent and the N_2H_4/Ni^{2+}ratios were 10 and 12, they also observed that particle size decreases with the increase of the reductant concentration (Wu and Chen.,2003; Bai *et al*., 2008).

The results revealed that NiNPs could be obtained in ethanol, even in the absence of a protective polymer. Additionally, it can be suggested that, ethanol might form a protective layer around the particle surface via the interaction of OH groups with

nickel atoms, preventing particle aggregation or agglomeration (Wu and Chen.,2003; Bai *et al*., 2008).

3.1.4 Thermogravimetry analysis (TGA) and differential scanning calorimetry (DSC).

Fig. 3.4 shows that the weight of nickel nanopowders stays constant or shows a very slight decrease (1.63% by weight) at temperatures below 270 °C. This is probably caused by the absorbed residues such as water and/or carbon dioxide as the samples were exposed to the atmosphere (Song *et al*., 2008). The NiNPs begin to show weight gain at ~409 °C in the thermogravimetric curve where a slight increase in the DSC curve is observed, an implication of oxidation occurs at this temperature. Comparing to the typical initial oxidation temperature of bulk nickel materials, ~ 600 °C, the oxidation of NiNPs occurs at a much lower temperature.

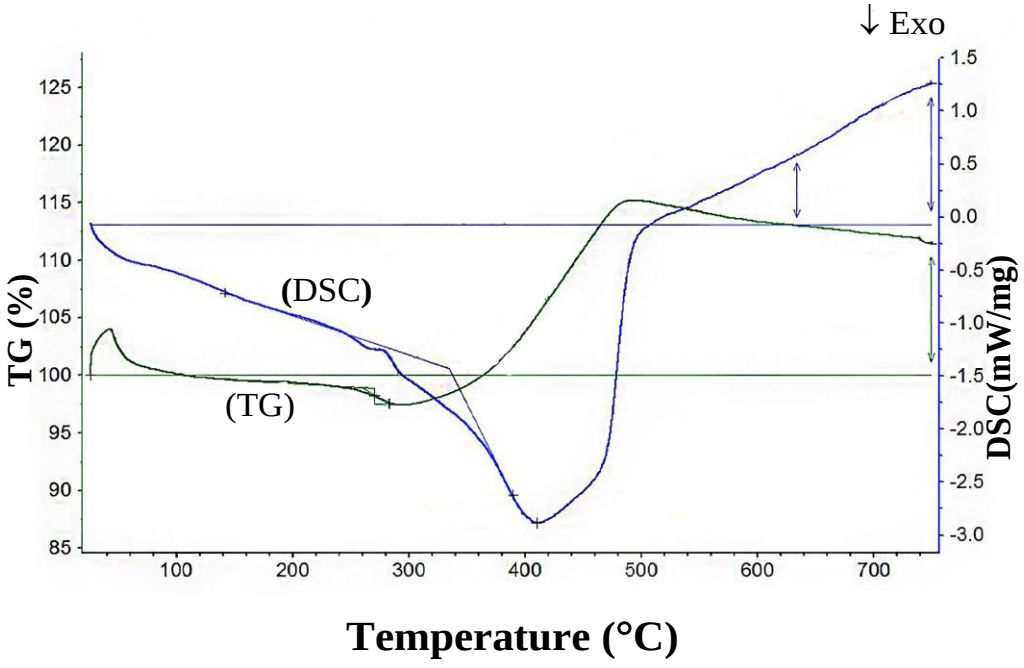

Fig. 3.4 Thermogravimetry analysis (TGA) and differential scanning calorimetry (DSC).

The fastest reaction occurs at ~ 410 °C where the DSC peak is detected due to the exothermic oxidation reaction, Song *et al* 2008 reported less temperature value (398 °C) and Harish and Kumar (2011) reported (313.11°C), presumably that slight difference can be attributed to the size of Nickel particles. A pronounced change in the oxidation kinetics, as observed from the slope decrease of the TGA curve, occurs at ~ 490 °C.

The final weight increase of this sample material is 11.44%, which is lower than the ideal weight increase of 27.3% for complete pure-nickel oxidation (Song *et al*., 2008). This can be attributed to a thin layer of amorphous oxide that formed before experiments.

Song *et al*. (2008) reported an experimental investigation of complete oxidation of NiNPs using simultaneous thermogravimetry analysis (TGA) and differential scanning calorimetry (DSC), their results were similar to those results, but with a slight decrease in oxidation temperature (398 °C) and higher value of final mass gain, presumably that slight decrease in their values because of the smaller particles size of their NiNPs, this assumption can be demonstrated by the empirical relationship between diameter and melting point Eq (3-2)

$$T_m = T_0\left(1 - {}^{1}/_{\mathrm{d}}\right) \quad \ldots\ldots (3\text{-}2)$$

where T_0 denotes the bulk melting point, *d* the diameter, T_m the melting point of the nanoparticle and the melting point is inversely related to the diameter(Van *et al*., 2020). Harish and Kumar (2011) studied the oxidation of NiONPs and similar results were reported. nanoparticles of average size 10-20 nm the oxidation began at about 313.11 °C and the weight gain increased linearly as the isothermal time lengthened. Bai *et al*. (2008) found that weight gain starts at 200 °C and becomes significant from 260 °C, indicating thermal oxidation of the obtained NiNPs began at about 200 °C. Compared with that reported by Chen and Zhou, 305 °C when the

particle size was 400 nm, in another study by Robinson *et al*. (2010) the mass increase due to oxidation of nickel started in between 320 °C and 360 °C and Astafyev *et al* (2020) reported ~ 415 °C. (Chen and Zhou, 2006.; Bai *et al*., 2008)

3.1.5 Fourier transform infra-red (FTIR) spectroscopy

Fig.3.5 shows the absorption band at around 550-600 cm^{-1} was the only peak observed, and it may be due to the metal nature (Chaudhary *et al*., 2015). in other hand, absence of peaks in other regions demonstrates the purity of prepared NiNPs and absence of residual organic compound such as hydrazine and ethanol.

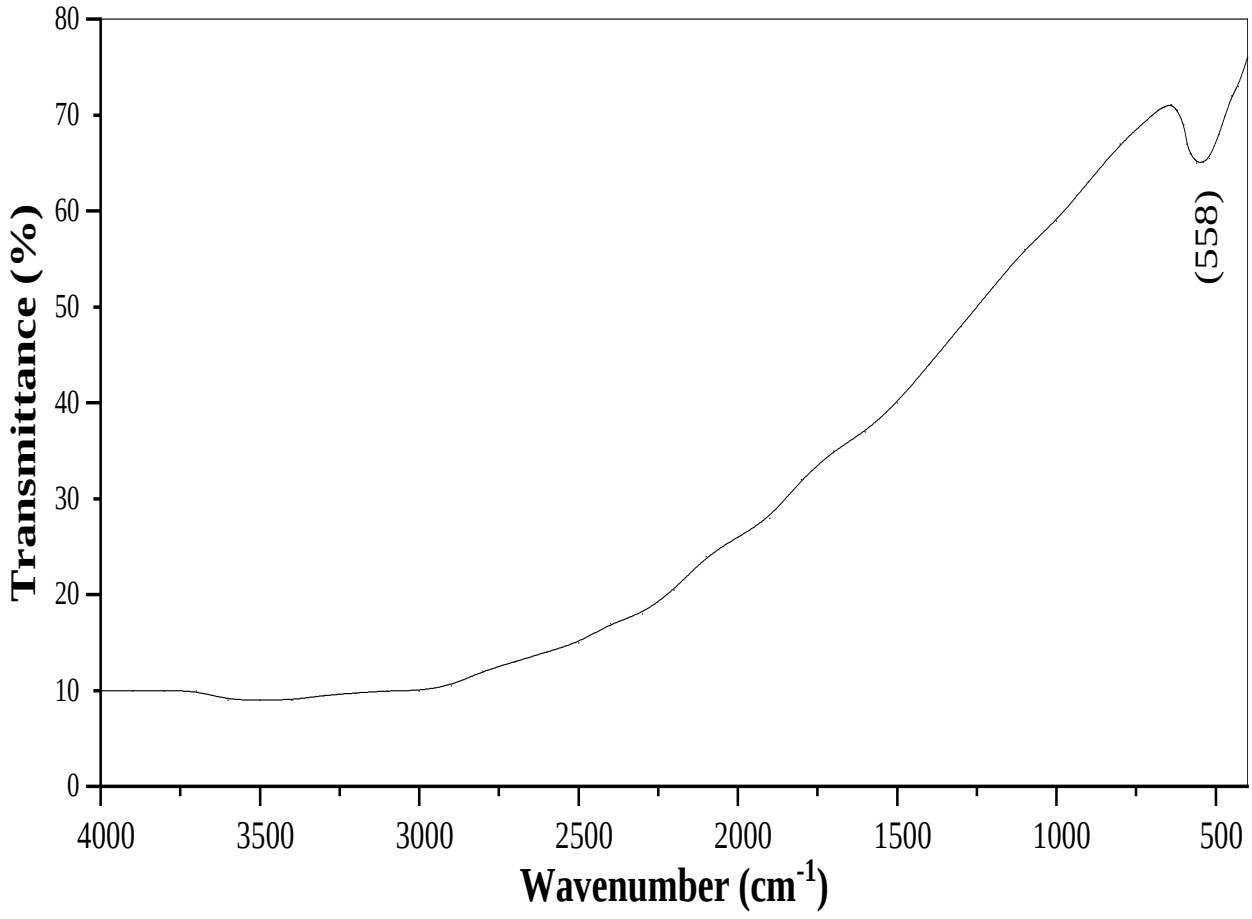

Fig.3.5 FT-IR spectra of NiNPs

3.2 Applications of NiNPs

3.2.1 Viscosity reduction of heavy crude oil.

Table 3.1. and Figs.3.6, 3.7 and 3.8. show the results of the reduction of heavy crude oil viscosity from 7128 mPa.s to 3495 mPa.s (51%) when 0.05 % (w/v) NiNPs was used, and it was evidenced by the change in the density from 0.9514 g/cm^3 to 0.9416 g/cm^3 and API number from 17.04 to 18.59 (9.0%) of the crude oil indicating the conversion of heavy component into lighter ones.

Table No. 3.1: Viscosity, density and API reduction results

	BS&W (%)		**Density (g/cm^3)**				**Viscosity @ 29 °C**	
Sample Name	Water (V%)	Sedi. (V%)	Density (50 °C)	SG API (15°C)	Density Rho (15.6 °C)	**API**	(mPa.s)	**Red. %**
Heavy crude oil (Blank)	4.00	0.00	0.9290	0.9530	0.9514	17.04	7128	0.0
1%Hydr.+ 3%Xylene	4.00	0.00	0.9278	0.9510	0.9502	17.23	6666	6.5
0.05%NiNPs+3%Xyl.	4.00	0.00	0.9190	0.9430	0.9416	18.59	3495	51.0
0.05%NiNPs+3%Xyl.+1 % Hydrazine	4.00	0.00	0.9170	0.9410	0.9397	18.89	3212	55.0

Similar results were obtained by many researchers, Desouky *et al*. (2013) found that the rate of viscosity reduction was 73 and 79 % for iron (III) dodecylbenzene sulfonate and nickel (II) dodecylbenzene sulfonate catalysts at temperature range of 150-175 °C. Cacciola *et al*. (1993) investigated the catalytic effect of oil soluble naphthene on aquathermolysis, the experimental result showed that Ni and Pt have being activity, selectivity and stability for dehydrogenation of cyclohexane and methylcyclohexane.

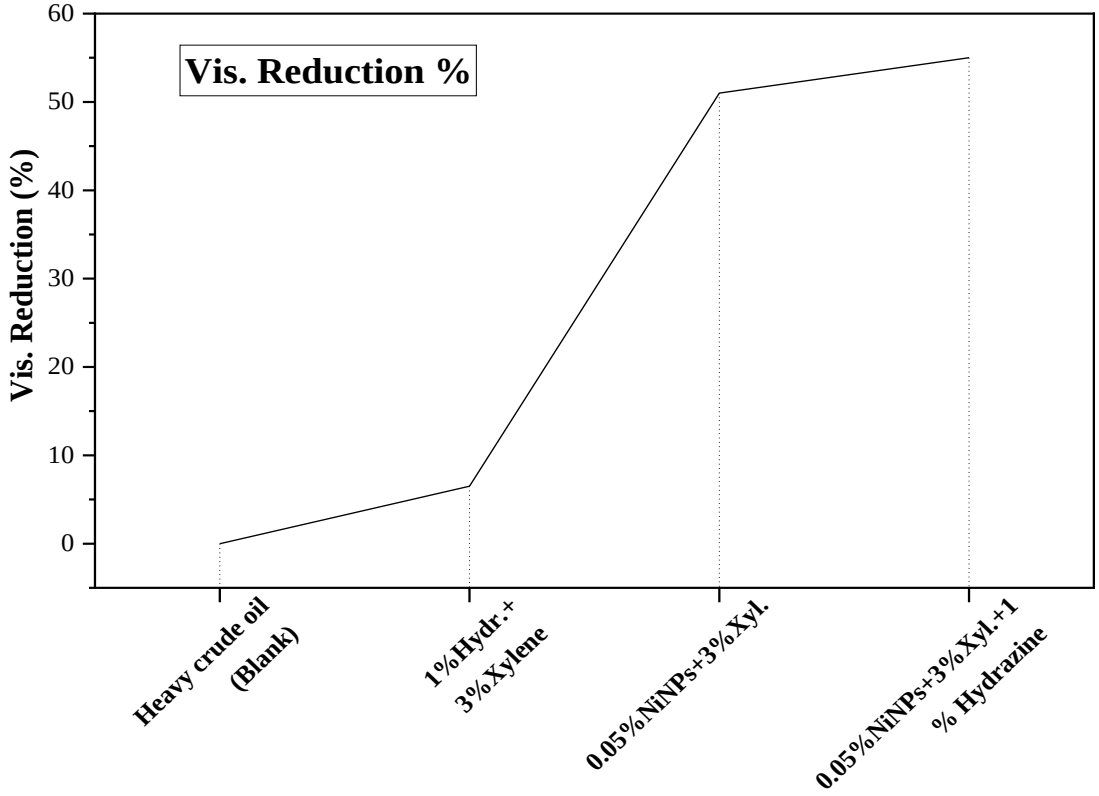

Fig.3.6 Heavy crude oil viscosity reduction %

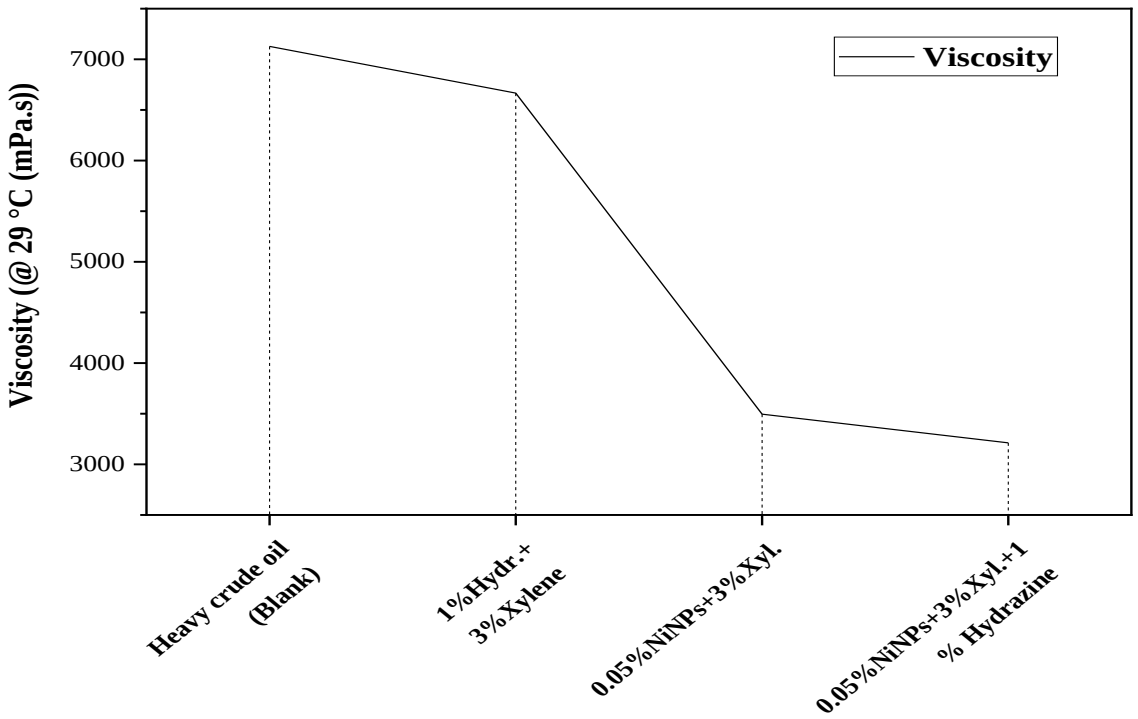

Fig.3.7 Heavy crude oil viscosity reduction

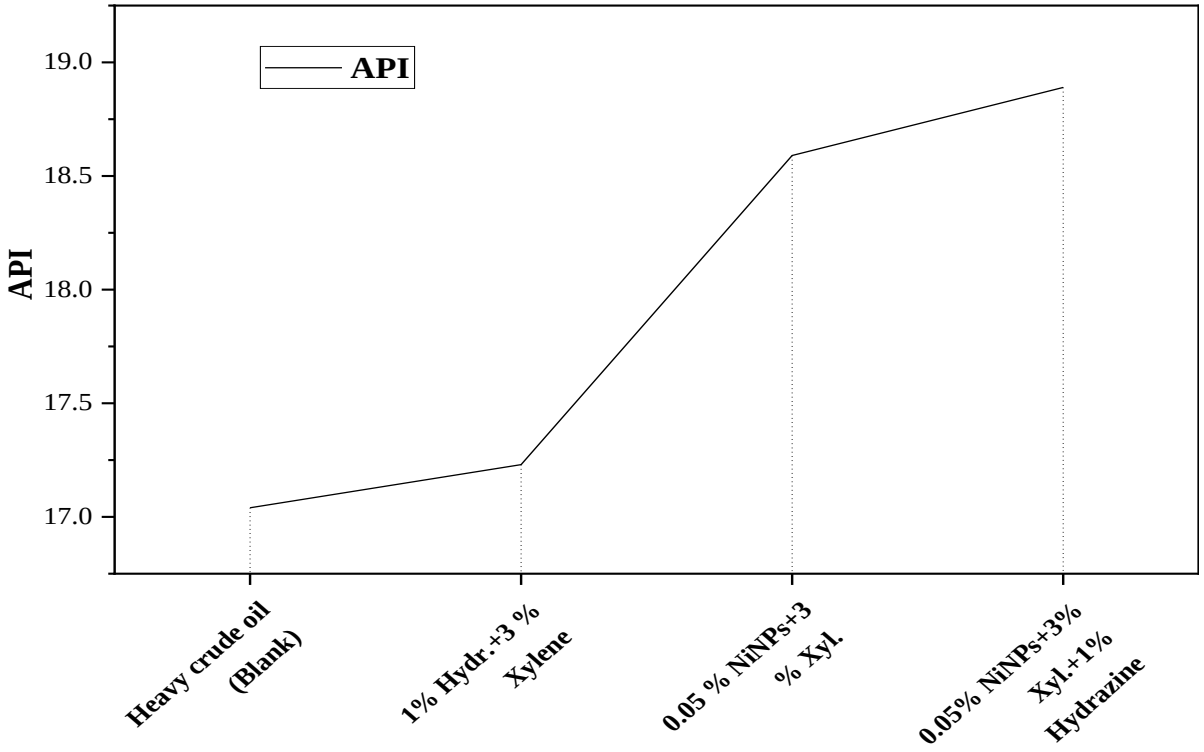

Fig.3.8 API reduction

It has been reported that added hydrogen donor additive is an effective way to enhance the viscosity reduction, e.g. tetralin can release free radical hydrogen, which can react with the active chains formed in the processes of aquathermolysis and restrain the polymerization, Lui and Fan (2002) found that adding 0.8% tetralin as a hydrogen donor could reduce crude oil viscosity up to 80 % at 240 °C for 24 h, but the product of tetralin and nanphthalene is poisonous to human beings and tetralin is very expensive, accordingly, it is important to find an alternative and non-toxic donor to enhance the reaction. Therefore, 1 % of hydrazine monohydrate as a hydrogen donor (Hu *et al*., 2016) was used for more investigations, and to demonstrate the effect of hydrogen donors on the reaction of the hydro aquathermolysis, according to the results obtained in table 3-1, 1 % hydrazine monohydrate and 0.05 % NiNPs increased the reduction of the heavy crude oil viscosity and the API up to 55.0 % and 10.8 %, respectively, while 51.0 % and 9.0

%, respectively, was achieved with only 0.05 % NiNPs and without hydrazine additive donor as hydrogen donor at 70 °C. In a similar study, Chen *et al*. (2016) employed methanol as a hydrogen donor additive in the reaction system, and they found that the viscosity was reduced further, with the increase in dosage of methanol. As the dosage of methanol reached 15.0% (weight percent of the heavy oil) the viscosity reduction ratio reached as high as 82.6% at 45 °C.

3.2.2 Produced water treatment using NiNPs

Table 3-2 in Fig. 3.9 are used to determine the required NiNPs dosage to the desirable treatment concentration. The remaining solution concentration changed on treatment with different weights of NiNPs. In addition, percentage removal of dissolved oil also increases with the increasing of NiNPs dose, and the maximum removal percentage of dissolved oil is 98 % (40 mg L^{-1}), and according to Kuwait Convention and (Red Sea region) this minimum discharge limit of dissolved oil in produced water is 100 mg L^{-1} maximum (Kuwait R.C.,1979)**.** An increasing trend in the adsorption capacity of NiNPs was noticed as shown in Fig. 3.10 because of its high affinity with dispersed oil. A similar result was obtained by Ko *et al.* 2(014), in their study, they used a magnetic nanoparticle assisted with a surfactant, however, the removal efficiency was 99.99 % of dispersed oil. Liang *et al.* (2015) investigated magnetic demulsification of single-layer oleic acid-coated magnetite

Table 3-2: Dispersed oil adsorption results on NiNPs

W (g)	C_i (mg L^{-1})	C_e (mg L^{-1})	q_e (mgg^{-1})	$1/C_e$	ln C_e	$1/q_e$	ln qe	Rem. %
0.01	550	157	3932	0.0064	5.0547	2.5E-04	8.28	71.5
0.02	550	100	2250	0.0100	4.6052	4.4E-04	7.72	81.8
0.03	550	71	1598	0.0142	4.2569	6.3E-04	7.38	87.2
0.04	550	54	1240	0.0185	3.9890	8.1E-04	7.12	90.2
0.05	550	40	1020	0.0250	3.6889	9.8E-04	6.92	92.7

(Fe_3O_4OA) nanoparticles as a demulsifier for cyclohexane-diluted crude oil-in-water nanoemulsions and under magnetic field, the highest removal was 98 %.

Functionalized and coated magnetic nanoparticles in certain processes was found to reach as high as 99.99 % in a study performed by (Simonsen *et al*., 2018).

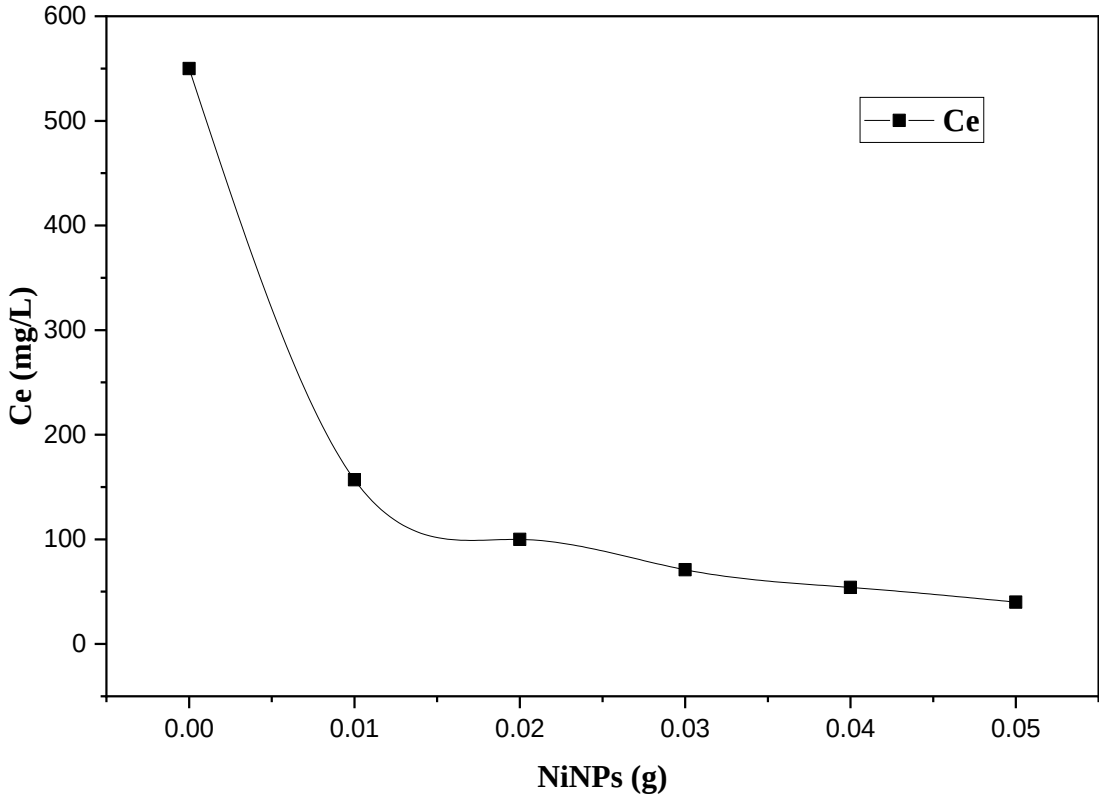

Fig. 3.9 The Effect of NiNPs on dispersed oil removal.

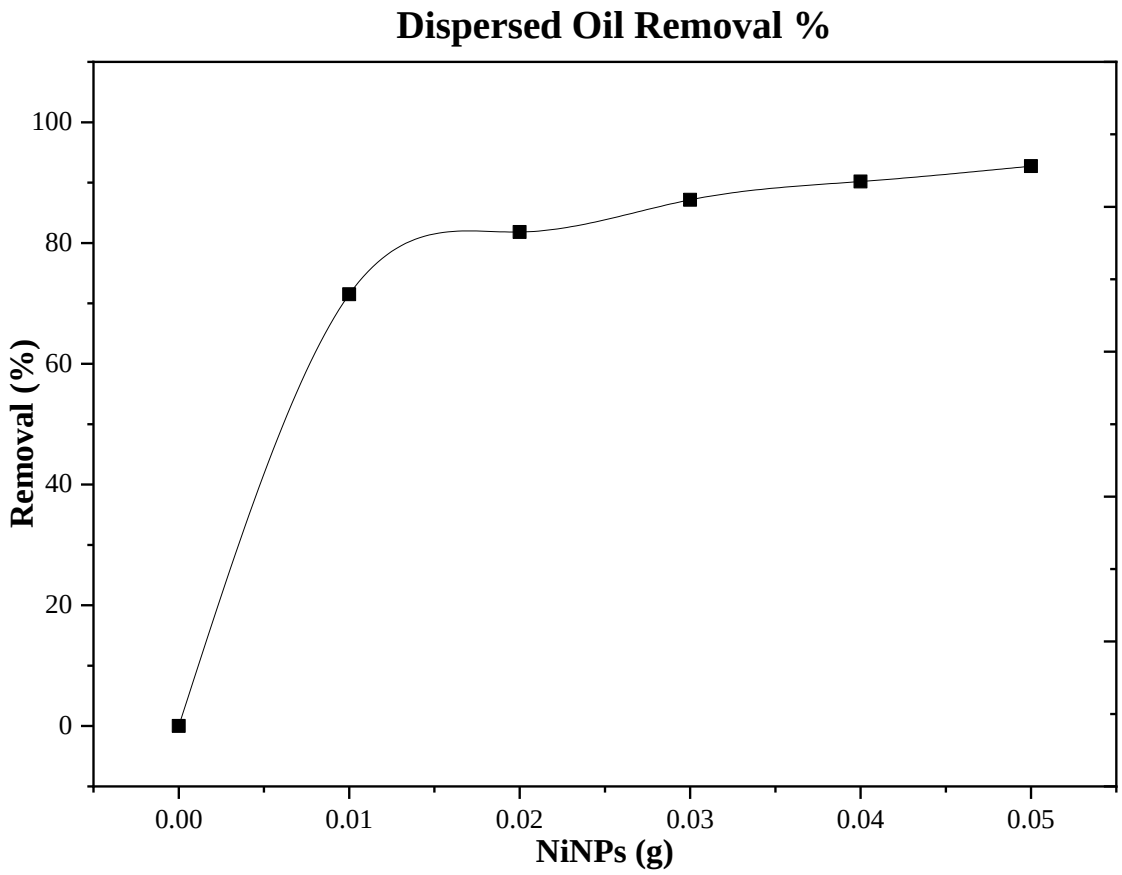

Fig. 3.10: The effect of NiNPs on dispersed oil removal.

3.2.3 Application of Langmuir's and Freundlich's models to dispersed oil adsorption

An adsorption isotherm provides useful information about adsorption capacity, binding affinity as well as the surface properties of the NiNPs which help understand the binding mechanism of adsorbate. Two theoretical models, Langmuir and Freundlich's isotherms were used to examine the adsorption behavior of NiNPs for dispersed oil uptake as shown in Fig.3.11 and 3.12. The Langmuir's isotherm describes the monolayer adsorption of pollutant onto the NiNPs surface having finite number of adsorption sites whereas Freundlich's isotherm supports that adsorption occurs on heterogeneous surface of the adsorbent (Sierra and Louvier., 2020). The results presented in table 3-2 and represented in Fig.3.11 and 3.12, demonstrate that Freundlich isotherm's was the best fitted because the value of linear regression

coefficient (R^2 = 0.98314) of this isotherm was observed to be higher than that with Langmuir's isotherm (R^2 = 0.9775). Maximum adsorption capacity of NiNPs for dispersed oil was found to be 22841mg g^{-1}. The values of separation factor (R_L) for NiNPs is less than one (0.670) which favor the adsorption phenomenon. In a similar study, Nickel nanoparticles encapsulated in porous carbon/carbon nanotube hybrids (Ni/PC-CNT) was used to remove organic dyes from aqueous solution, the maximum adsorption capacity obtained in this study was (898 mg g^{-1}) (Jin *et al*., 2018). In another research, NiNPs adsorbent was biosynthesized using *Ocimum sanctum* leaf extract. the maximum adsorption capacities in Langmuir isotherm were found to be 0.454, 0.615, 0.273, 0.795 and 0.645 mg g^{-1} for CV, EY, OR, NO_3^- and SO_4^{2-} respectively, and R^2 = 0.870 for all dyes and pollutants (Pandian *et al*.,2015). Data in Table 3-2 presented in Fig 3.12, was found to fit Freundlich isotherm model and the constants k and 1/n are 24.24 and 1.005 respectively, mentioned in the literature review is that 1/n <1. The position and slope of the isotherm line revealed the performance of the NiNPs, the representation of the experimental data by Freundlich equation resulted in a nearly linear curve with (R^2=0.9832)

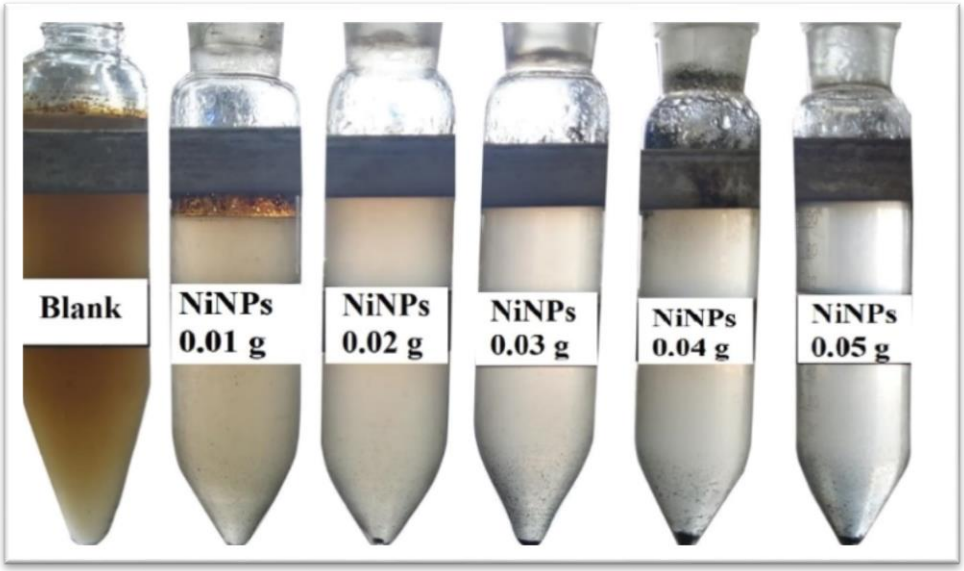

Pic. 3.1: **The effect of NiNPs on dispersed oil removal**

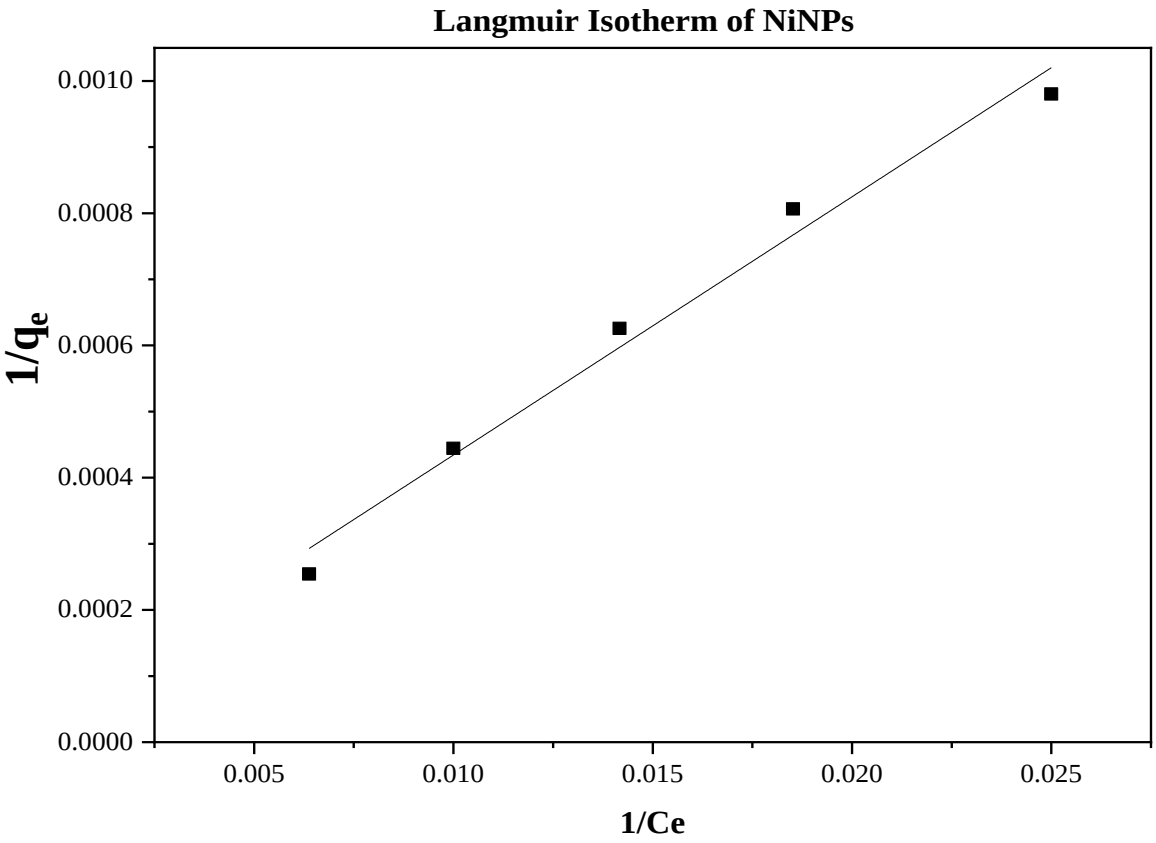

Fig.3.11 Langmuir's isotherm plots for the adsorption of dispersed oil onto NiNPs.

Table.3-3 Langumir's isotherm parameters for the removal of dispersed oil by NiNPs.

Intercept	Slop	q_{max} (mg g^{-1})	K_L (L mg^{-1})	R_L	R^2
0.000044	0.03905	22841	0.001121	0.670	0.9775

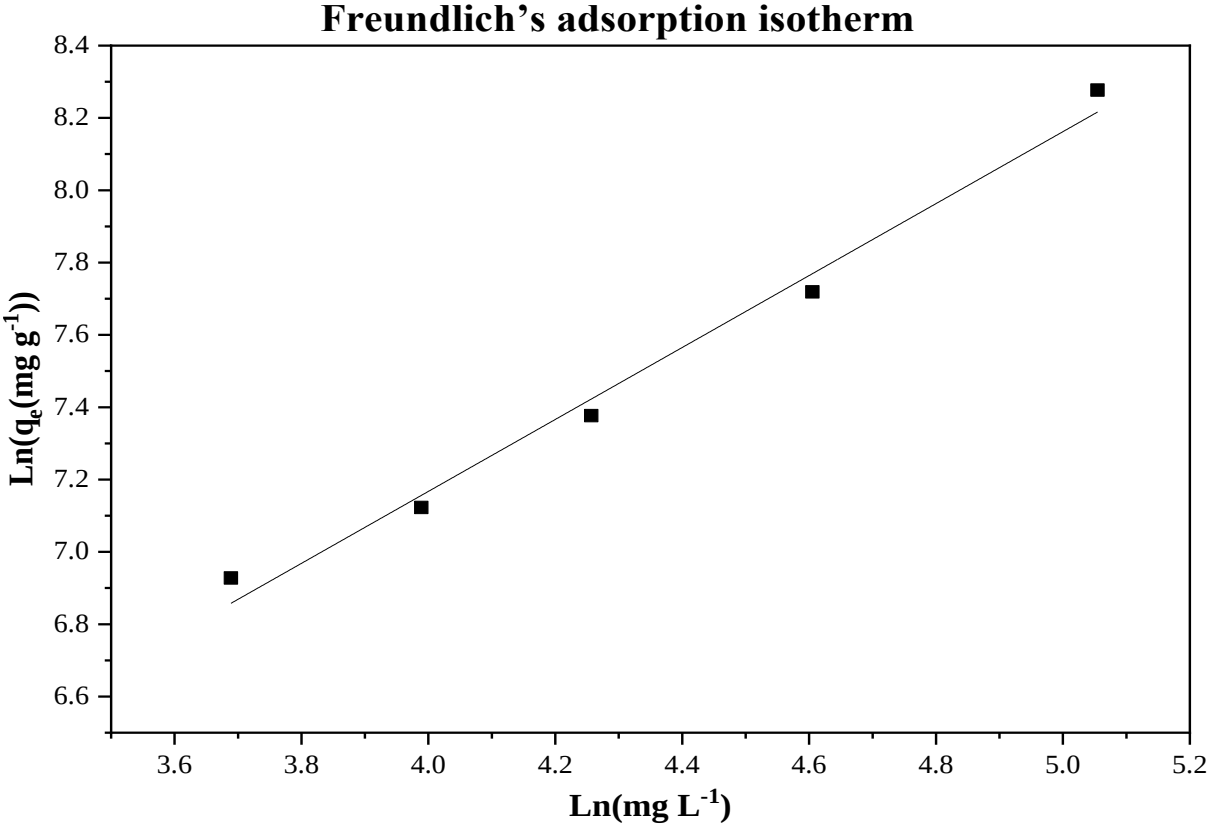

Fig.3.12: Freundlich's isotherm plots for the adsorption of dispersed oil onto NiNPs

Table 3-4: Freundlich's isotherm parameters for the removal of dispersed oil by NiNPs

1/n	K_f	R^2
1.005	24.24	0.98314

3.3 Conclusion

- Nickel nanoparticles (NiNPs) were synthesized using hydrazine monohydrate as a reductant with 10:1 and 15:1 (N_2H_2/N^{+2}) molar ratios in alkaline solution using ethanol as a solvent at 60 °C.
- Prepared NiNPs were characterized using XRD, TEM, TGA-DSC and FTIR, results show that pure NiNPs has an average particles size of 50-90 nm.
- NiNPs were used to reduce heavy oil viscosity, results revealed that NiNPs could reduce heavy oil viscosity by (51%) and API number from (9.0%) with 0.05 % NiNPs at 80 °C.
- NiNPs were also used for produced water treatment as an adsorbent, results obtained showed that maximum removal percentage of dispersed oil is 98 %.
- In Langmuir's isotherm, adsorption capacity (q_{max}) of the NiNPs was 22,841 mg g^{-1} for dispersed oil. constants K_L, R_L and R^2 were 0.001121 (L mg^{-1}), 0.670 and 0.9775respectively.
- Freundlich's isotherm constants k and 1/n were 24.24 and1.005 ,respectively, and R^2 was 0.9832.

3.4 Recommendations

- To investigate different reductant type with different molar ratios.
- Intensive study in the mechanism of viscosity reduction.
- Apply NiNPs on sewage and waste water treatment.
- Testify the biological activity of NiNPs.
- Combine NiNPs with organic deoiler (demulsifiers) to increase their separation efficiency.

References:

Abhijit Kar, Ajoy Kumar Ray, (2014). "Synthesis of nano-spherical nickel by templating hibiscus flower petals", *Journal of Nanoscience and Nanotechnology*, **2**(2): 17-20.

Ádám, A., Szabados, M., Polyákovics, Á., Musza, K., Kónya, Z., Kukovecz, Á., Si pos, P. and Pálinkó, I. (2019). "The Synthesis and Use of Nano Nickel Catalysts". *Journal of Nanoscience and Nanotechnology*, **19**(1):453-458.

Ádám, A.A., Szabados, M., Varga, G., Papp, Á., Musza, K., Kónya, Z., Kuk ovecz, Á., Sipos, P. and Pálinkó, I., (2020)." Ultrasound-assisted hydrazine reduction method for the preparation of nickel nanoparticles, physicochemical characterizeationand catalytic application in Suzuki-Miyaura cross-coupling react - ion". *Nanomaterials*, **10**(4):632.

Alboudwarej, H & Felix, J & Taylor, *et al*. (2006)." Highlighting heavy oil". *Oilfield Review*.**18**: 34-53.

Alomair OA, Matar KM, Alsaeed YH, (2015). "Experimental study of enhanced-heavy-oil recovery in Berea sandstone cores by use of nanofluids applications". *SPE Reserv. Eval. Eng.***18**:387–399.

Alramadhan, S.A. and Hammud, H.H., (2021). "Graphene nickel silica supported nanocomposites as an efficient purifier for water treatment". *Applied Nano science*, **11**(1):.273-291.

Astafyev, A., Lysenko, E., Surzhikov, A., Nikolaev, E. and Vlasov, V., (2020). "Thermomagnetometric analysis of nickel–zinc ferrites". *Journal of Thermal Analysis and Calorimetry*, **142**(5):1775-1781.

Ayub, A., Raza, Z., Majeed, M., Tariq, M. and Irfan, A., (2020). "Development of sustainable magnetic chitosan biosorbent beads for kinetic remediation of arsenic contaminated water". *International Journal of Biological Macro molecu les*, **163**:603-617.

Bagaria, H.G., Yoon, K.Y., Neilson, B.M., Cheng, V., Lee, J.H., Worthen, A .J ., Xue, Z., Huh, C., Bryant, S.L., Bielawski, C.W. and Johnston, K.P., (2013). "Stabilization of iron oxide nanoparticles in high sodium and calcium brine at high temperatures with adsorbed sulfonated copolymers". *Langmuir* ,**29** (10) :3195-3206.

Bai, L., Yuan, F. and Tang, Q., (2008). "Synthesis of nickel nanoparticles with uniform size via a modified hydrazine reduction route". *Materials Letters*, **62** (15) :2267-2270.

Baig, N., Kammakakam, I. and Falath, W., (2021). "Nanomaterials: a review of synthesis methods, properties, recent progress, and challenges". *Materials Adv ances*, **2**(6):1821-1871.

Burda, C., Chen, X., Narayanan, R., and EI-Sayed, M.A. (2005) "Chemistry an -d properties of nanocrystals of different shapes". *Chem. Rev*., **105**: 1025–1102.

Cacciola, G., Aristov, Y.I., Restuccia, G. and Parmon, V.N., (1993). "Influence of hydrogen-permeable membranes upon the efficiency of the high-temperature chemical heat pumps based on cyclohexane dehydrogenation-benzene hydrogenation reactions". *International journal of hydrogen energy*, **18**(8):673-680.

Chaudhary, R.G., Tanna, J.A., Gandhare, N.V., Rai, A.R. and Juneja, H.D., (2015). "Synthesis of nickel nanoparticles: microscopic investigation, an efficient catalyst and effective antibacterial activity". *Adv. Mater. Lett*, **6**(11):990-998.

Chen, G., Yuan, W., Su, H., Zhang, J., Gu, X., Bai, Y. and Jeje, A., (2016). "Methanol enhanced catalytic viscosity-reduction of heavy oil by transition metal-Mannich base complex under low temperature". *Russian Journal of Applied Chemistry*, **89**(11):1853-1860.

Chen, H., Wang, J., Huang, D., Chen, X., Zhu, J., Sun, D., Huang, J. and Li, Q ., (2014). "Plant-mediated synthesis of size-controllable Ni nanoparticles with alfalfa extract". *Materials Letters*, **122**:166-169.

Chen, R.Y. and Zhou, K.G., (2006). "Preparation of ultrafine nickel powder by wet chemical process". *Transactions of Nonferrous Metals Soc. of China*, **16** (5):1223-1227.

Chen, Y., He, J., Wang, Y. and Li, P., (2010)." GC-MS used in study on the mechanism of the viscosity reduction of heavy oil through aquathermolysis catalyzed by aromatic sulfonic H3PMo12O40". *Energy*, **35**(8):3454-3460.

Chen, Y., Peng, D.L., Lin, D. and Luo, X., (2007)."Preparation and magnetic properties of nickel nanoparticles via the thermal decomposition of nickel organ -o metallic precursor in alkylamines". *Nanotechnology*,**18** (50):505-703.

Chen, Y., Wang, Y., Wu, C., & Xia, F. (2008). "Laboratory experiments and field tests of an amphiphilic metallic chelate for catalytic aquathermolysis of heavy oil". *Energy & Fuels*, **22**(3): 1502-1508.

Clark, P.D. and Hyne, J.B., (1990). "Studies on the chemical reactions of heavy oils under steam stimulation condition". *Aostra J Res*, **29**(6):29-39.

Clark, P.D., Hyne, J.B. and Tyrer, J.D., (1983). "Chemistry of organosulphur comp ound types occurring in heavy oil sands: 1. High temperature hydrolysis and

thermolysis of tetrahydrothiophene in relation to steam stimulation processes" . *Fuel*, **62**(8):959-962.

Clark, P.D., Hyne, J.B. and Tyrer, J.D., (1984). "Some chemistry of organo sulphur compound types occurring in heavy oil sands Influence of pH on the high temperature hydrolysis of tetrahydrothiophene and thiophene". *Fuel*, **63** (1):125-128.

Clesceri, L., Eaton, A. and Greenberg, A., (1998). *Standard methods for the examination of water and wastewater*. Washington, D.C.: APHA/AWWA/WEF.

Desouky, S., Betiha, M., Badawi, A., Ghanem, A. and Khalil, S., (2013). "Catalytic aquathermolysis of Egyptian heavy crude oil". *International Journal of Chemical and Molecular Engineering*, **7**(8):638-643.

Desta, M., (2013). "Batch Sorption Experiments: Langmuir and Freundlich Iso therm Studies for the Adsorption of Textile Metal Ions onto Teff Straw (Eragrostis tef) Agricultural Waste". *Journal of Thermodynamics*, **2013**:1-6.

Drexler, K. E. (1986). *Engines of creation*. Anchor.

Dusseault, M.B., (2001), "Comparing Venezuelan and Canadian heavy oil and tar sands". *Canadian International Petroleum Conference*. Petroleum Society of Canada.

Dutta, A. and Dolui, S. K., (2011), "Tannic acid assisted one step synthesis route for stable colloidal dispersion of nickel nanostructures", *Applied Surface Science*, **257**(15):6889-6896.

Ec.europa.eu.(2018).“ Nanomaterials in REACH and CLP – Environment *“European Commission*.[online] Available at: http://ec.europa.eu/environment/ che micals/nanotech/studies/index_en.htm [Accessed 16 Dec. 2018].

Elshawaf, M., (2018), “September. Investigation of graphene oxide nanoparticles effect on heavy oil viscosity. *In SPE Annual Technical Conference and Exh ibition*. Society of Petroleum Engineers.

Eluri, R. and Paul, B. (2012). Synthesis of Nickel nanoparticles by hydrazine reduction: mechanistic study and continuous flow synthesis. *Journal of Nanopa - rticle Research*, **14**(4):800.

Eluri, R. and Paul, B., (2012). “Microwave assisted greener synthesis of nickel nanoparticles using sodium hypophosphite”. *Materials Letters*, **76**:36-39.

Fakhru’l-Razi, A., Pendashteh, A., Abdullah, L.C., Biak, D.R.A., Madaeni, S.S. and Abidin, Z.Z., (2009). “Review of technologies for oil and gas produced water treatment”. *Journal of hazardous materials*, **170**(2-3):530-551.

Fan, H., Zhang, Y. and Lin, Y., (2004). “The catalytic effects of minerals on aquathermolysis of heavy oils”. *Fuel*, **83**(14-15):2035-2039.

Feyman, R., (1959). “There’s plenty of room at the bottom: an invitation to entera new field of physics”. In conférenceprononcée au congrèsannuel de l’A merican Physical Society, *California Institute of Technology*, **29**: 5-22.

Franco CA, Lozano MM, Acevedo S, Nassar NN, Cortes FB, (2016). “Effects of resin I on asphaltene adsorption onto nanoparticles: a novel method for obtaining asphaltenes/resin isotherms”. *Energy Fuels*, **30**:264–272.

Gatoo, M., Naseem, S., Arfat, M., Mahmood Dar, A.,Qasim, K. and Zubair, S. (2014).” Physicochemical Properties of Nanomaterials: Implication in Associated Toxic Manifestations”. *BioMed Research International*,**2014**:1-8.

Ghanbarabadi, H. and Khoshandam, B., (2020). “Thermogravimetric synthesis of Ni nanoparticles with varied morphologies and particle sizes”. *Particulate Science and Technology*, **38**(6):685-693.

Goia, D., (2004). “Preparation and formation mechanisms of uniform metallic particles in homogeneous solutions”. *Journal of Materials Chem*,**14**(4):45 1.

Hamedi Shokrlu Y, Babadagli T., (2014). “Kinetics of the in-situ upgrading of heavy oil by nickel nanoparticle catalysts and its effect on cyclic-steam-stimulation recovery factor”. *SPE Reserv. Eval. Eng*, **17**:355–364.

Hamedi Shokrlu, Y. and Babadagli, T., (2010),“Effects of nano-sized metals on viscosity reduction of heavy oil/bitumen during thermal applications”. In *Canadian Unconventional Resources and International Petroleum Conference*. Society of Petroleum Engineers.

Hamedi Shokrlu, Y. and Babadagli, T., (2013). “In-situ upgrading of heavy oil/ bitumen during steam injection by use of metal nanoparticles: A study on in-situ catalysis and catalyst transportation”. *SPE Reservoir Evaluation &Engineering*, **16**(03):333-344.

Harish, K., Renu, R. and Kumar, S.S., (2011), “Synthesis of Nickel Hydroxide Nanoparticles by Reverse Micelle Method and Its Antimicrobial Activity”, *Res earch J. of Chemical Sci.*, **1**:42-48.

Hascakir,B., Babadagli, T., Akin, S., 2008. Experimental and numerical model ing of heavy-oil recovery by electrical heating. In: Proceedings of the SPE/ PS/ CHOA, International Thermal Operations and Heavy Oil Symposium. Calgary Canada, October 20–23.

Hashemi, R., Nassar, N.N. and Pereira lmao, P., (2013).” Enhanced heavy oil recovery by in situ prepared ultradispersed multi/metallic nanoparticles: A study of hot fluid flooding for Athabasca bitumen recover”. *Energy & Fuels*, **27**(4):2194-2201.

Hernández-Varela, J.D., Chanona-Pérez, J.J., Benavides, H.A.C., Sodi, F.C.and Vicente-Flores, M., (2021).” Effect of ball milling on cellulose nanoparticles structure obtained from garlic and agave waste”. *Carbohydrate Polymers*, **255** :117347.

Hu, J., Ding, Y., Zhang, H., Wu, P. and Li, X., (2016). “Highly effective Ru/ C MK-3 catalyst for selective reduction of nitrobenzene derivatives with H2O as solvent at near ambient temperature”. *RSC advances*, **6**(4):3235-3242.

Hyne, J. B., Greidanus, J. W., Tyrer, J. D., Verona, D., Rizek, C., Clark, P. D. ,& Koo, J. (1982). “Aquathermolysis of heavy oils”. *Revista Tecnica Intevep* ,**2**(2): 87-94.

Iskandar, F., Dwinanto, E., Abdullah, M. and Muraza, O., (2016). “Viscosity reduction of heavy oil using nanocatalyst in aquathermolysis reaction” *Powder and Particle Journal*, **33**:3-16.

Iskandar, F., Dwinanto, E., Abdullah, M. and Muraza, O., (2016). "Viscosity reduction of heavy oil using nanocatalyst in aquathermolysis reaction". *KONA Powder and Particle Journal*, **2016**:005.

Iso.org.(2018).*Nanomaterials*.[online]Availableat:https://www.iso.org/obp/ui/ #iso:std: iso:ts:80004:-1 :ed-2:v1:en [Accessed 16 Dec. 2018].

Jia, F.L., Zhang, L.Z., Shang, X.Y. and Yang, Y., (2008). "Non- Aqueous Sol-Gel Approach towards the Controllable Synthesis of Nickel Nanospheres, Nano -wires, and Nanoflowers". *Advanced Materials*, **20**(5):1050-1054.

Jin, L., Zhao, X., Qian, X. and Dong, M., (2018). "Nickel nanoparticles encapsulated in porous carbon and carbon nanotube hybrids from bimetallic metal-organic-frameworks for highly efficient adsorption of dyes". *Journal of colloid an d interface science*, **509**:245-253.

K. Aslan, I. Gryczynski, J.Malicka, E.Matveeva, J. R. Lakowicz, and C. D. Ge ddes,(2005),"Metal-enhanced fluorescence:an emerging tool in biotechnology," *Current Opinion in Biotechnology*, **16**: 55–62.

Khanna, P.K., More, P.V., Jawalkar, J.P. and Bharate, B.G., (2009)." Effect of reducing agent on the synthesis of nickel nanoparticles". *Materials Letters*, **63** (16) :1384-1386.

Ko, S., Prigiobbe, V., Huh, C., Bryant, S.L., Bennetzen, M.V. and Mogensen, K., (2014), "Accelerated oil droplet separation from produced water using magnetic nanoparticles". In *SPE Annual Technical Conference and Exhibition*. Society of Petroleum Engineers.

Lai, T.L., Lee, C.C., Wu, K.S., Shu, Y.Y. and Wang, C.B., (2006)" Microwave enhanced catalytic degradation of phenol over nickel oxide". *Applied Catalysis B: Environmental*, **68**(3-4):147-153.

Lashanizadegan, A., Ayatollahi, S. and Homayoni, M. (2008). "Simultaneous heat and fluid flow in porous media: case study: steam injection for tertiary oil recovery". *Chemical Engineering Communications*, **195**(5):521-535.

Lenggoro, I.W., Itoh, Y., Iida, N. and Okuyama, K.,(2003)" Control of size and morphology in NiO particles prepared by a low-pressure spray pyrolysis" . *Materials research bulletin*, **38**(14):1819-1827.

LI, W., ZHU, J. and QI, J. (2007). Application of nano-Nickel catalyst in the viscosity reduction of Liaohe extra-heavy oil by aquathermolysis. *Journal of Fuel Chemistry and Technology*, **35**(2):176-180.

Li, Z., Han, C. and Shen, J. (2006). Reduction of Ni^{2+} by hydrazine in solution for the preparation of Nickel nano-particles. *Journal of Materials Science*,**41** (11):3473-3480.

Liang, J., Du, N., Song, S. and Hou, W., (2015). "Magnetic demulsification of diluted crude oil-in-water nanoemulsions using oleic acid-coated magnetite nanoparticles". *Colloids and Surfaces A: Physicochemical and Engineering Aspects*, **466:**197-202.

Liu, S., Tam, S.K. and Ng, K.M., (2021). "Dual-reductant synthesis of nickel nanoparticles for use in screen-printing conductive paste". *Journal of Nanoparticle Research*, **23**(3):1-12.

Liu, Y. and Fan, H., (2002)". The effect of hydrogen donor additive on the viscosity of heavy oil during steam stimulation". *Energy & fuels*, **16**(4):842-846.

Luo, Z.Y., Chen, K.X., Wang, Y.Q., Wang, J.H., Mo, D.C. and Lyu, S.S., (2016). "Superhydrophilic nickel nanoparticles with core–shell structure to decorate copper mesh for efficient oil/water separation". *The Journal of Physical Chemistry*, **120**(23):12685-12692.

M. Cahay (2001). "Quantum Confinement VI: Nanostructured Materials and Devices : Proceedings of the International Symposium". *The Electrochemical Society*. ISBN 978-1-56677-352-2.

Mariam A. A. , M. Kashif, S. Arokiyaraj ,(2014), "Bio-synthesis of NiO and Ni nanoparticles and their characterization", *Digest Journal of Nanomaterials and Biostructures*, **9**(3):1007–1019.

Matteo, C., Candido, P., Vera, R. and Francesca, V., (2012). "Current and future nanotech applications in the oil industry". *American Journal of Applied Sciences*, **9**(6):784-793.

Mendes, P. M. , S. Jacke , K. Critchley , *et al*. (2004) "Gold Nanoparticle Patterning of Silicon Wafers Using Chemical e - Beam Lithography ". *Langmuir* ,**20**:3766 – 8.

Meneses, C.T., Flores, W.H., Garcia, F. and Sasaki, J.M., (2007). "A simple route to the synthesis of high-quality NiO nanoparticles". *Journal of Nanoparticle Research*, **9**(3):501-505.

Montes, D., Henao, J., Taborda, E.A., Gallego, J., Cortés, F.B. and Franco, C.A., (2020)." Effect of Textural Properties and Surface Chemical Nature of Silica

Nanoparticles from Different Silicon Sources on the Viscosity Reduction of Heavy Crude Oil". *ACS omega*, **5**(10):5085-5097.

Nguyen, C.M., Frias Batista, L.M., John, M.G., Rodrigues, C.J. and Tibbetts, K.M., (2021). "Mechanism of Gold–Silver Alloy Nanoparticle Formation by Laser Coreduction of Gold and Silver Ions in Solution". *The Journal of Physical Chemistry* B, **125**(3):907-917.

Olah GA, DeMember JR, Shen J. (1973), "Electrophilic reactions at single bonds. X. Hydrogen transfer, alkylation, and alkylolysis of alkanes with methyl and ethyl fluoroantimonate". *Journal of the American Chemical Society*. **95**(15):4952-6.

Omole O., Olieh M.N., Osinowo T., (1999), "Thermal visbreaking of heavy oil", *Fuel*, **78** (12): 1489-1496.

Owen, J., & Floyd, J. (1981). "Enhanced oil recovery methods". *Oil Gas Petro - chem Equip* **27**(1)**:**11.

Pandey, A. and Manivannan, R. (2015). "A Study on Synthesis of Nickel Nano - particles Using Chemical Reduction Technique". *Recent Patents on Nano -medicine*, **5**(1):33-37.

Pandian, C.J., Palanivel, R. and Dhananasekaran, S., (2015). "Green synthesis of nickel nanoparticles using Ocimum sanctum and their application in dye and pollutant adsorption". *Chinese journal of Chemical engineering*, **23**(8):1307-1315.

Park, J.W., Chae, E.H., Kim, S.H., Lee, J.H., Kim, J.W., Yoon, S.M. and Choi, J.Y., (2006)." Preparation of fine Ni powders from nickel hydrazine complex" . *Materials Chemistry and Physics*, **97**(2-3):371-378.

Peng, J., Liu, Q., Xu, Z. and Masliyah, J., (2012). "Novel magnetic demulsifier for water removal from diluted bitumen emulsion". *Energy & fuels*, **26**(5) :2705-2710.

Poole Jr, C. P., & Owens, F. J. (2003)." Introduction to nanotech.". *John Wiley & Sons*.

Raja, P.M.V. & Barron, A.R., (2021). "Thermal Analysis". Available at: https: //chem.libretexts.org/@go/page/55853 [Accessed May 11, 2021].

Ramirez-Garnica, M.A., Hernandez Perez, J.R., Cabrera-Reyes, M.D.C., Schacht-Hernandez, P. and Mamora, D.D., (2008), "Increase oil recovery of heavy oil in combustion tube using a new catalyst based on nickel ionic solution". *International Thermal Operations and Heavy Oil Symposium*. Society of Petroleum Engineers.

Ramsden, J. J. (2018). "What is Nanotechnology", *Applied Nanotech.* ,**1** :3–13.

Rao, C.N.R., Kulkarni, G.U., Thomas, P.J., and Edwards, P.P. (2002) Size dependent chemistry: properties of nanocrystals. *Chem. Eur. J.*, **8**:28–35.

Ravindhranath, K. and Ramamoorty, M., (2017)," Nickel Based Nano Particles as Adsorbents in Water Purification Methods-A Review". *Oriental Journal of Chemistry*, **33**(4):1603.

Robinson, P., Arun, V., Manju, S., Aniz, C. and Yusuff, K., (2010). "Oxidation kinetics of nickel nano crystallites obtained by controlled thermolysis of diaquabis (ethylenediamine) nickel (II) nitrate". *Journal of thermal analysis and calorimetry*, **100**(2):733-740.

Roduner, E. (2006). "size matters: why nanomaterials are different". *Chemical society reviews*, **35**(7): 583-592.

Shaban, S., Dessouky, S., Badawi, A.E.F., El Sabagh, A., Zahran, A. and Mousa, M., (2014). "Upgrading and viscosity reduction of heavy oil by catalytic ion ic liquid". *Energy & fuels*, **28**(10):6545-6553.

Shokrlu, Y.H. and Babadagli, T., (2014). "Viscosity reduction of heavy oil/ bitumen using micro-and nano-metal particles during aqueous and non-aqueous thermal applications". *Journal of Petroleum Science and Engineering*, **119**:210-220.

Shokrlu, Y.H., Maham, Y., Tan, X., Babadagli, T. and Gray, M., (2013). "Enhancement of the efficiency of in situ combustion technique for heavy-oil recovery by application of nickel ions". *Fuel*, **105**:397-407.

Sierra-Trejo, P.V., Guibal, E. and Louvier-Hernández, J.F., (2020). "Arsenic sorption on chitosan-based sorbents: Comparison of the effect of molybdate and tungstate loading on As (V) sorption properties". *Journal of Polymers and the Environment*, **28**(3):934-947.

Simonsen, G., Strand, M. and Øye, G., (2018). "Potential applications of magnetic nanoparticles within separation in the petroleum industry". *Journal of Petroleum Science and Engineering*, **165**:488-495.

Song, P., Wen, D., Guo, Z.X. and Korakianitis, T., (2008). "Oxidation investingation of nickel nanoparticles". *Physical Chemistry Chemical Physics,* **10** (33) :5057-5065.

Subramanie, P.A., Padhi, A., Ridzuan, N. and Adam, F., (2020). "Experimental study on the effect of wax inhibitor and nanoparticles on rheology of Malaysian crude oil". *Journal of King Saud University-Engineering Sciences*, **32** (8): 479-483.

Sudhasree, S., Shakila Banu, A. Brindha, P. and Kurian, G.A., **(**2014), "Synthesis of nickel nanoparticles by chemical and green route and their comparison in respect to

biological effect and toxicity", *Toxicological and Environmental Chemistry*, **96**(5):743-754.

Sun, Y.P., Li, X.Q., Zhang, W.X. and Wang, H.P., (2007). "A method for the preparation of stable dispersion of zero-valent iron nanoparticles". *Colloids and Surfaces A: Physicochemical and Engineering Aspects*, **308**(1-3):60-66.

Thema, F.T., Manikandan, E., Gurib-Fakim, A. and Maaza, M., (2016). "Single phase Bunsenite NiO nanoparticles green synthesis by Agathosma betulina natural extract". *Journal of alloys and compounds*, **657**:655-661.

Thoma, G.J., Bowen, M.L. and Hollensworth, D., (1999). "Dissolved air precipitation/solvent sublation for oil-field produced water treatment". *Separation and Purification Technology*, **16**(2):101-107.

Tientong , J., Garcia, S., Thurber, C. and Golden, T., (2014). "Synthesis of Nickel and Nickel Hydroxide Nanopowders by Simplified Chemical Reduction". *Journal of Nanotechnology*, **2014**:1-6.

USEPA. (2004). "Code of Federal Regualtions. Title 40 Protection of Environment". Part 435.12. Effluent limitations guidelines representing the degree of effluent reduction attainable by the application of the best practicable control technology cureently available (BPT).

van Teijlingen, A., Davis, S.A. and Hall, S.R., (2020). "Size-dependent melting point depression of nickel nanoparticles". *Nanoscale Advances*, **2** (6) :2347-2351.

Vaseem, M., Tripathy, N., Khang, G. and Hahn, Y.B.,(2013). "Green chemistry of glucose-capped ferromagnetic hcp-nickel nanoparticles and their reduced toxicity". *RSC advances*, **3**(25):9698-9704.

Wang, D. Z., Wille, U., &Juaristi, E. (Eds.). (2017). Encyclopedia of Physical Organic Chemistry., John Wiley & Sons, Inc. ISBN 978-1-118-46858-6.

Wu, S.H. and Chen, D.H., (2003). "Synthesis and characterization of nickel nanoparticles by hydrazine reduction in ethylene glycol". *Journal of Colloid and Interface Science*, **259**(2):282-286.

Wu, X., Xing, W., Zhang, L., Zhuo, S., Zhou, J., Wang, G. and Qiao, S., (2012)." Nickel nanoparticles prepared by hydrazine hydrate reduction and their application in supercapacitor". *Powder technology*, **224**:162-167.

Wu, Z., Munoz, M. and Montero, O. (2010). "The synthesis of Nickel nanop -articles by hydrazine reduction". *Advanced Powder Technology*, **21**(2):165-168.

Xu, W., Liew, K.Y., Liu, H., Huang, T., Sun, C. and Zhao, Y., (2008). "Mic rowave-assisted synthesis of nickel nanoparticles". *Materials letters*, **62**(17-18): 2571-2573.

Yoon, K.Y., Kotsmar, C., Ingram, D.R., Huh, C., Bryant, S.L., Milner, T.E. and Johnston, K.P., (2011). "Stabilization of superparamagnetic iron oxide nanoclusters in concentrated brine with cross-linked polymer shells". *Langmuir* ,**27**(17): 10962-10969.

Yoon, K.Y., Li, Z., Neilson, B.M., Lee, W., Huh, C., Bryant, S.L., Bielawski, C.W. and Johnston, K.P., (2012)." Effect of adsorbed amphiphilic copolymers on the interfacial activity of superparamagnetic nanoclusters and the emulsification of oil in water". *Macromolecules*, **45(**12):5157-5166.

Zabala, R.F.C.A., Franco, C.A. and Cortés, F.B., (2016), "Application of nanofluids for improving oil mobility in heavy oil and extra-heavy oil: a field test". *improved oil recovery conference*. Society of Petroleum Engineers.

Zhang, G., Li, J., Zhang, G. and Zhao, L. (2015). "Room-Temperature Synthesis of Ni Nanoparticles as the Absorbent Used for Sewage Treatment". *Advances in Materials Science and Engineering,* **2015**:1-4.

Zhe, Z. and Yuxiu, A., (2018). "Nanotechnology for the oil and gas industry an overview of recent progress". *Nanotechnology Reviews*, **7**(4):341-353.

Zhu, L., Cui, J., Zhang, H., Ruan, L., Ma, N., Zou, L., Deng, T., Chen, B.H. and Xiao, Q., (2019). "Room- Temperature Morphology- Controlled Synthesis of Nickel and Catalytic Properties of Corresponding Catalysts. Ru/Ni" *Chem CatChem*, **11**(13):3109-3116.